Journal of Environmental Analytical Chemistry

Abugu et al., J Environ Anal Chem 2015, 2:6
DOI: 10.4172/2380-2391.1000165

Research Article Open Access

Preparation and Characterization of Activated Carbon Produced from Oil Bean (Ugba or Ukpaka) and Snail Shell

Abugu HO*, Okoye PAC, Ajiwe VIE, Omuku PE and Umeobika UC

Department of Pure and Industrial Chemistry, Nnamdi Azikiwe University, Awka, Anambra State, Nigeria

Abstract

Two agro wastes were selected and carbonized at 600°C for 45 min and 800°C for 30 min and each was divided into three different portions. Each portion was activated with HCl, H_2SO_4 and H_3PO_4 as activating agents. The activated carbons were characterized for some important parameters such as pH, ash content, nitrogen, carbon content, sulphur, fat, fibre, protein, moisture content, carbohydrate, oxygen, hydrogen, sodium, potassium and pore volume. Wastewater from battery industry was collected and treated with the activated carbons with a view to determining the extent of the heavy metal adsorption ability. The results of the characterization shows pH range of 6.71 to 6.82, while the pore volume ranged from 3.9×10^{-5} to 2.4×10^{-5} m^3/g for Oil Bean activated carbon and 8.7×10^{-6} to 6.2×10^{-6} m^3/g for Snail shell activated carbon. The percentage yield of activated carbon before activation is 25.79 to 27.27 for Oil Bean and 61.85 to 86.11% for Snail shell activated carbon. FTIR results shows a surface reorganization of the activated carbon with a formation of new functional groups after chemical activation. The adsorption data generated fitted well into the Freundlich isotherm model since most values of the determination coefficient (R^2) >0.500 indicating a heterogeneous adsorption of heavy metals from aqueous solution. It was observed also that those carbon activated with H_3PO_4 were better adsorbents in most of the activated carbons produced irrespective of the heavy metals, followed by those activated with HCl while those activated with H_2SO_4 were the least. The ANOVA indicates that there exist a positive significance relationship between the reliability factor (R^2) and the Langmuir constants in almost all the activated carbon types produced. So also it was for Freundlich isotherm constants except few of them. This study has shown that activated carbon produced from oil Bean shell and Snail Shell can compete favourably with traditional activated carbons in treating industrial waste especially from battery industries using HCL, H_2SO_4 and H_3PO_4 as activating agents.

Keywords: Adsorption; Activated carbon; Heavy metals; Treatment; Snail shell

Introduction

Industrial and municipal waste water can contain many impurities, which are divided into different pollutant groups (among others dissolved and undissolved substances, easily degradable organic substances, persistent organic substances, plant nutrients, heavy metals, and salts). The aim of effluent treatment is the elimination of these undesired impurities and the restoration of natural water quality. The contaminations are usually pre-cleaned with other treatment processes such as flocculation, sedimentation adsorption and/or biological treatment. The activated carbon is usually used in a last processing step to remove the most difficult impurities like heavy metals other pharmaceutical micro pollutants. The activated carbon used for cleaning (granular or powder) has to fulfill many different tasks: removal of organic-chemical substances and colorants, reduction of trace substances like chemicals or pharmaceuticals, enormous decrease of residual Chemical Oxygen Demand. Human activities such as mining and associated smelting, burning of fossil fuels, and industrial uses of mercury (Hg) in paints, batteries, medicine, and dentistry have significantly increased the global reservoir of atmospheric metals since the beginning of the industrialized period [1]. High concentrations of heavy metals have been found in sediments and fish in the vicinity of small-scale mining activities using amalgamation as their main technique. The concentration in most fish fillets in these areas exceeds the recommendations of the United States Food and Drug Agency [2] A major concern about the increasing background concentration of heavy metals in the environment is that any inorganic form (less toxic) can be converted into organic form, especially methyl-mercury, one of the most toxic compounds known to humans. Therefore the main objective of the problem is to treat waste water before discharging to water source, thus decreasing the threat and deterioration to the environment and promising better sustainability of the environment. There are many technologies that have been developed for the purification and treatment of wastewater and among them is adsorption. But the hitch is the cost of establishing an adsorption column for this purpose. This research tends to device a cost effective means of producing activated carbon from cheap agricultural wastes.

Materials and Methods

List of apparatus

The following apparatus was used in the course of the research: Digital pH meter (Labtech 4620), Weighing balance (Metler MP301), Digital Muffle furnace (Labtech 201), Burette, retort stand**,** Sample bottles, Beakers, Pestle and Crucible, Platinium Crucible, 1.18 mm Mesh, Dessicator, Thermometer, Filter paper, Fume Cupboard, Funnels, FTIR (Buck 530 FTIR), SEM (Aspex 3020 PSEM2), stop watch, kjehdal flask, Measuring cylinder, Petri dish.

List of reagents

Hydrochloric acid (HCl), Phosphoric acid (H_3PO_4), Sulphuric acid (H_2SO_4), sodium hydroxide (NaOH), Deionized water, Barium Chloride ($BaCl_2$), Cadmium chloride monohydrate ($CdCl_2.H_2O$), manganese sulphate monohydrate ($MnSO_4.H_2O$), Nickel Chloride hexahydrate ($NiCl_2.6H_2O$), Lead Nitrate ($Pb(NO_3)_2$), Selenium powder and Perchloric acid $HClO_4$.

***Corresponding author:** Abugu HO, Department of Pure and Industrial Chemistry, Nnamdi Azikiwe University, Awka, Anambra State, Nigeria, Tel: 2348038847309; E-mail: abunze@gmail.com

Received October 14, 2015; **Accepted** October 27, 2015; **Published** November 07, 2015

Citation: Abugu HO, Okoye PAC, Ajiwe VIE, Omuku PE, Umeobika UC (2015) Preparation and Characterization of Activated Carbon Produced from Oil Bean (Ugba or Ukpaka) and Snail Shell. J Environ Anal Chem 2: 165. doi: 10.4172/2380-2391.1000165

Sampling and pre-sample treatments

Precursor (raw material) selection for the production of activated carbon was obviously the first step of the research Conventionally, activated carbon is produced from carbonaceous source material such as wood, peat, coal, and wastes of vegetable origin (example-nutshells, fruit stones). Today, one promising approach for the production of cheap and efficient activated carbon is the reuse of agricultural waste produced at Rural, Municipal or Industrial activities. The usage of waste materials is especially important due to its mass production and waste reuse so as to make our environment safer. The two types of agricultural wastes chosen as precursor were: Oil bean (Pentaclethra Macrophylla) shell (Ugba or Ukpaka in Igbo land) and Snail shell. The Oil bean shell was collected from Obollo Afor in Enugu State while the Snail Shell was collected from Marina road, Eket, Akwa Ibom State (Figures 1-4). Dirt was removed from the samples after which they were washed and sun dried.

Carbonization and activation

The procedure by Grigis [3] with slight modifications was used. The Shell was removed, washed, dried and crushed using locally made grinder. This was sieved to 1.18 mm and carbonized at 800°C for 30 mins and 600°C for 45 mins. 75 g of the carbonized sample was mixed with 20% of three different solvents (H_2SO_4, HCl and H_3PO_4) solution at a ratio of 1:1 (Acid: char). This impregnation at 80°C was done with continuous stirring for 2 hours. After that, the sample was then filtered, washed with deionized water and dried overnight at 120°C in oven. Activated carbons were gradually cooled to room temperature. It was washed severally using deionized water until the washing deionized water had a pH of 7.0. The prepared activated carbons were dried at 120°C overnight, cooled and stored for further studies.

Figure 1: Oil bean.

Figure 2: Smashed Oil Bean shell.

Figure 3: Snail Shells.

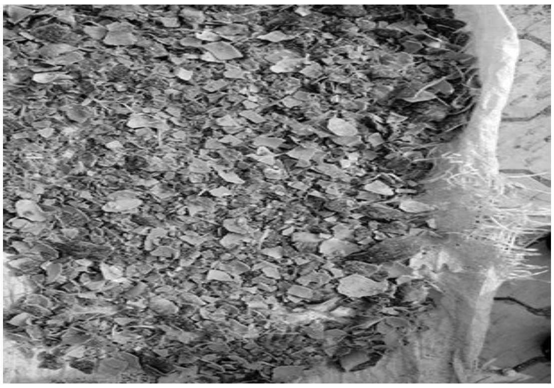

Figure 4: Smashed Snail Shells.

Determination of the carbonization yield: The carbonization yield was determined as follows:

Yield (%) = weight of carbon produced/weight of raw sample used × 100

Carbon content determination [4]

Procedure:

Empty Platinum Crucible was washed, dried and the weight was noted.

Exactly 2 g of wet sample was weighed into the Platinum Crucible and placed in a Muffle Furnace at 850°C for 3 hours.

The sample was cooled in a desiccator after burning and weighed.

Calculations:

$$\%\,\text{ash content} = \frac{W_3 - W_1}{W_2 - W_1} \times \frac{100}{1}$$

Where

W_1=weight of empty Platinum Crucible

W_2=weight of Platinum Crucible and sample before burning

W_3=weight of Platinum and carbon.

Nitrogen content determination [4]

Principle: the method is the digestion of sample with hot concentrated sulphuric acid in the presence of a metallic catalyst (Selenium powder). Organic nitrogen in the sample is reduced to ammonia. This is retained in the solution as ammonium sulphate. The solution is made alkaline, and then distilled to release the ammonia. The ammonia is trapped in dilute acid and then titrated.

Procedure: Exactly 1 g of each sample was weighed into a 30 ml kjehdal flask (this was gently done to prevent the sample from touching the walls of the Flask) and then the flasks were closed (stoppered) and shaken. Then 1 g of the kjeldahl catalyst mixture was added. The mixture was heated in a digestion rack under fire until a clear solution was seen. The clear solution was then allowed to stand for 30 minutes in order for it to cool. After cooling about 100 ml of deionized water was added to avoid caking and then transferred to the kjeldahl digestion apparatus. A 500 ml receiver flask containing 5 ml of boric acid indicator was placed under a condenser of the distillation apparatus so that the tap was about 20 cm inside the solution. The 10 ml of 40% sodium hydroxide was added to the digested sample in the apparatus and distillation commenced immediately until distillation reaches the 35 ml mark of the receiver flask, after which it was titrated to pink color using 0.01N Hydrochloric acid.

Calculation:

% Nitrogen=Titre value × 0.01 × atomic mass of Nitrogen × 4

Where 0.01=normality of the acid.

Sulphur content determination [5]

Digestion of samples: 10 g of the dried sample was Weighed into a digestion flask and 20 ml of the acid mixture (650 ml of concentrated HNO_3; 80 ml Perchloric acid; 20 ml concentrated H_2SO_4) was added**.** The flask was heated until a clear digest was obtained. The digest was then diluted with distilled water to the 250 ml mark. Appropriate dilutions were then made for each element to be determined. Sulphate was analysed according to APHA standard method [6].

Procedure: A 250 cm^3 of the sample was evaporated to dryness on a dish. The residue was moistened with a few drops of Conc. HCl and 30 cm^3 distilled water. The mixture was boiled and then filtered. The dish was rinsed and the filter paper washed with distilled water severally and both filtrate and washings added together. This was heated to boiling and then 10 cm^3 of 10% $BaCl_2$ solution was added, drop by drop with constant stirring. The mixture was digested for about 30 minutes, filtered and the filter paper washed with warm distilled water. It was then ignited, cooled and weighed in a pre-weighed crucible.

Calculation: mg/dm^3 Sulphur=mg $BaSO_4$ × 411.5 cm^3 of water sample

Determination of heavy metal concentration

Heavy metal concentration was carried out using Varian AA240 Atomic Absorption Spectophtometer. The samples were prepared for AAS analysis according to Adrian [5]. 2 g of the dried sample was weigh into a digestion flask and 20 ml of the acid mixture (650 ml conc HNO_3; 80 ml Perchloric acid; 20 ml conc H_2SO_4) was added. It was heated until a clear digest was obtained. The digest was diluted to the 100 ml mark with deionized water.

Proximate analysis methods

Moisture content: Procedure: A petri-dish was washed and dried in the oven

- Exactly 2 g of the sample was weighed into the petri dish
- The weight of the petri dish and sample was recorded before drying in the oven
- The petridish and sample were put in the oven for 30 minutes and the weight was noted
- The drying procedure was continued until a constant weight was obtained

$$\%\,\text{moisture content} = \frac{W_1 - W_2}{\text{weight of sample}(2\,g)} \times 100$$

Where W_1=weight of petri dish and sample before drying

$W_{2=}$weight of petri dish and sample after drying

Carbohydrate determination (Differential method)

100-(%Protein+%Moisture+%Ash+%Fat+%Fiber)

Ash Content [4]: The ash content of sample is the inorganic residue remaining after the organic matter has been burnt off.

Procedure: Empty Platinum Crucible was washed, dried and the weight was recorded.

Exactly 2 g of the wet sample was weighed into the Platinum Crucible and placed in the Muffle Furnace at 500°C for 3 hours.

The sample was cooled in a Dessicator after burning and it was weighed and weight recorded.

Calculations:

$$\%\,\text{ash content} = \frac{W_3 - W_1}{W_2 - W_1} \times 100$$

Where:

W_1=weight of empty platinum crucible

W_2=weight of platinum crucible and sample before burning

W_3=weight of platinum and ash.

Determination of the Percent fixed carbon

Percentage fixed carbon=100-% ash content

Crude fibre determination

2 g of sample was de-fat with petroleum ether (this is done if the fat content was more than 10%). It was boiled under reflux for 30 minutes with 200 ml of a solution containing 1.25 g of H_2SO_4 per 100 ml of solution. The solution was filtered through linen on a fluted funnel. It was washed with boiling water until the washings were no longer acid. The residue was then transfers to a beaker and boiled for 30 minutes with 200 ml of a solution containing 1.25 g of Carbonate free NaOH per 100 ml.

The final residue was filtered through a thin but close pad of washed and ignited asbestos in a Gooch crucible. The Gooch crucible was dried in an electric oven and weighed. It was incinerated, cooled and then weighed. The loss in weight after incineration × 100 is the percentage of crude fibre.

$$\%\,\text{crude fibre} = \frac{\text{weight of fibre}}{\text{weight of sample}} \times 100$$

Determination of crude fat (Soxhlet fat extraction method)

This method is carried out by continuously extracting a sample with non-polar organic solvent such as petroleum ether for about 1 hour or more.

Procedure: A 250 ml clean boiling flasks was dried in oven at 105-110°C for about 30 minutes. It was transferred into a desiccator and allows to cool**.** It was labeled and weighed**.** The boiling flask was filled with about 300 ml of petroleum ether (boiling point 40-60°C)**.** The extraction thimble was plugged lightly with cotton wool**.** The soxhlet apparatus was assembled and allowed to reflux for about 6 hours**.** The thimble was removed with care and petroleum ether was collected draining into a container for re-use. The flask was removed and dried when the flask were almost free of petroleum ether at 105°C-110°C for 1 hour. It was transferred from the oven into a dessicator and allowed to cool, then weighed.

$$\%\,\text{fat} = \frac{\text{weight of Flask} + \text{oil} - \text{weight of Flask}}{\text{weight of sample}} \times 100$$

Determination of crude proteins [4]

Principle: The method is the digestion of sample with hot concentrated sulphuric acid in the presence of a metallic catalyst. Organic nitrogen in the sample is reduced to ammonia. This is retained in the solution as ammonium sulphate. The solution is made alkaline, and then distilled to release the ammonia. The ammonia is trapped in dilute acid and then titrated.

Procedure: Exactly 1 g of sample was weighed into a 30 ml kjehdal flask (gently to prevent the sample from touching the walls of the flask) and then the flasks were stoppered and shaken. Then 1 g of the kjedahl catalyst mixture was added. The mixture was heated cautiously in a digestion rack under fire until a clear solution was seen. The clear solution was then allowed to stand for 30 minutes and allowed to cool. After cooling, about 100 ml of deionized water was added to avoid caking and then 50 ml was transferred to the kjedahl distillation apparatus. A 100 ml receiver flask containing 5 ml of 2% boric acid and indicator mixture containing 5 drops of Bromocresol blue and 1 drop of methylene blue was placed under a condenser of the distillation apparatus so that the tap was about 20 cm inside the solution. 5 ml of 40% sodium hydroxide was added to the digested sample in the apparatus and distillation commenced immediately until 50 drops gets into the receiver flask, after which it was titrated to pink colour using 0.01N Hydrochloric acid.

Calculations: % Nitrogen=Titre value × 0.01 × 14 × 4

% Protein=% Nitrogen × 6.25

Determination of the adsorption efficiency

Stock solution of heavy metals was prepared by dissolving required quantity of Analar grade salts in deionized water. The salts used are cadmium chloride monohydrate ($CdCl_2.H_2O$), manganese sulphate monohydrate ($MnSO_4.H_2O$), nickel Chloride hexahydrate ($NiCl_2.6H_2O$), lead nitrate ($Pb(NO_3)_2$), Cobalt Chloride Hexahydrate ($CoCl_2.6H_2O$) for Cd(II), Mn(II), Ni(II), Pb(II), and Co(II) respectively, for the preparation of stock solution. The stock solution was further diluted with deionized water to desired concentration for obtaining the test solutions. NaOH was used for pH adjustments. The method by Grigis and Co. [3] with slight modification was used to study the adsorption capacity of each activated carbon prepared at different temperature and time from each of the agro waste. Dose of Activated Carbon was 2 g, Volume of Aqueous Solution used 10 ml, Different Initial Heavy Metal Concentration were prepared for different metal ranging from 35 mg/l to 150 mg/l, pH 7, Temperature was about room temperature, Contact Time 24 hours, Agitation Speed 120 rpm.

Adsorption Efficiency=C_0-C/C_0 × 100

C=concentration at equilibrium heavy metal

C_0=initial concentration of the heavy metal

Isotherm studies (Freundlich and Langmuir Isotherms)

The batch technique was selected to obtain equilibrium data because of its simplicity. Batch adsorption was performed at the same temperatures and initial Heavy Metal (HM) concentrations to obtain equilibrium isotherms. For isotherm studies, adsorption experiments was carried out by shaking 1 g of activated carbon samples with 100 ml flasks filled with 10 ml of HM solution at a concentration range 35 mg/l to 150 mg/L at a fixed temperature in a thermostated shaker bath for a known period of time. After equilibrium the suspension was filtered and the metal solution was then analyzed using AAS (Varian AA240). In order to obtain the adsorption capacity, the amount of ions adsorbed per mass unit of activated carbon sample (mg/g) was evaluated using the following expression:

$q_e=(C_0 - C_e)V/m$

Where q_e is the amount adsorbed at equilibrium (mg/g), C_0 is the initial metal ions concentration (mg/L), C_e is the equilibrium metal ions concentration (mg/L), V is the volume of the aqueous phase (L), and m is the amount of the activated carbon used.

Determination of pore volume

1 g of each activated carbons was immersed in water and boiled for 15 minutes in order to displace air from the pores of the activated carbons. The samples were superficially dried and reweighed. The pore volume was calculated from the difference in weight (dw) divided by the density of water (e) at room temperature.

Pore Volume=dw/e_{t25}

Results and Discussion

The proximate analysis of the samples was carried out (Table 1), and it was observed that the pH values of the samples ranged from 6.71 for OBAC and 6.82 for Snail shell indicating slightly neutral samples. It was also observed that OBAC had higher sulphur content (37035 mg/g). Also, the percentage ash, fat, fiber, nitrogen and protein contents were relatively low for both samples which are comparable to literature values [7,8]. Oil Bean had higher moisture content, 56.5% but recorded low percentage carbohydrate unlike its counterpart. The elemental analysis of the samples (Table 2), showed that Snail Shell recorded the highest carbon content (45.33%), indicating that it may be a good adsorbent. From Table 3, percentage yield after carbonization, we observe that Oil Bean had a low percentage yield after carbonization having recorded percentage yield below 50%, but snail shell had a percentage yield of 61.85% and 86.11% for the carbonization temperature of 800°C and 600°C respectively. This is in line with other studies [9]. This is also an evidence of the high carbon content recorded by snail shell in the elemental analysis presented in Table 2. It can also be observed that the percentage yield at a higher temperature is lower than that at lower

Sample	pH	Sulphur (Mg/g)	% Ash	% fat	% fibre	% N_2	% protein	% moisture	% Carbohydrate
Oil bean Shell	6.71	37.035	1.50	9.00	25.50	0.392	2.45	56.5	5.05
Snail Shell	6.82	20.575	4.00	6.00	24.00	0.56	3.5	5.5	57.40%

Table 1: The Proximate Analysis of the Samples.

Sample	Oil Bean	Snail Shell
Carbon (%)	19.61	45.33
Hydrogen (mg/g)	18.55	17.28
Oxygen (mg/g)	12.33	11.66
Sodium (ppm)	1.158	4.326
Potassium (ppm)	19.238	15.722

Table 2: The Elemental Analysis of the Samples.

Sample	800°C for 30 Min (%)	600°C for 45 Min (%)
Oil Bean	25.79	27.27
Snail Shell	61.85	86.11

Table 3: Percentage Yield after Carbonization.

Sample	800°C/30 Min (%)			600°C/45 Min (%)		
	H_2SO_4	HCl	H_3PO_4	H_2SO_4	HCl	H_3PO_4
Oil Bean	74.59	68.42	76.02	61.85	66.40	89.32
Snail shell	74.52	79.80	98.15	83.85	92.35	98.21

Table 4: Percentage Yield after Chemical Activation.

Activated Carbon Type	Initial Pb Conc. (mg/g)	Amount Adsorbed (mg/g)
OBAC/600°C/HCl	17.95	2.90
OBAC/600°C/H_2SO_4	17.95	4.77
OBAC/600°C/H_3PO_4	17.95	2.89
OBAC/800°C/HCl	17.95	3.69
OBAC/800°C/H_2SO_4	17.95	3.52
OBAC/800°C/H_3PO_4	17.95	0.47
SSAC/600°C/HCl	17.95	0.90
SSAC/600°C/H_2SO_4	17.95	0.11
SSAC/600°C/H_3PO_4	17.95	0.02
SSAC/800°C/HCl	17.95	0.88
SSAC/800°C/H_2SO_4	17.95	0.40
SSAC/800°CH_3PO_4	17.95	0.03

Table 5: Heavy Metal Concentration in Waste Water Samples from Ibeto Battery Industries and its treatment with Activated Carbons Prepared.

temperature even when carbonized at a longer period. This is because increase in temperature resulted in more volatile components of the precursor materials being lost, and hence decreases in percentage yield [9]. After chemical activation, the percentage yield (Table 4) was very high in all the samples at the temperatures used, though it was better for $H_3PO_{4,}$ in both conditions. The activation time does not influence the yield remarkably, relative to the activation temperature. The percentage yield of Palm Kernel activated at 800°C with H_3PO_4 and $ZnCl_2$ as activating agent as reported by Abechi 46.33% [9]. The waste water collected from Ibeto Battery factory (Nnewi) was analyzed for Pb concentration. The waste water was also treated with the various type of activated carbons produced and the result is as shown in Table 5. From the result it could be deduced that all the prepared activated carbons were good Pb adsorbents. The adsorption capacity of OBAC for Pb on waste water ranged from 0.47 to 4.77, while that of SSAC 0.02 to 0.90. This shows that when Oil Bean and Snail shell is carbonized at 800°C/600°C and activated with H_2SO_4, HCl or H_3PO_4, it can serve as a good adsorbent for the treatment of waste water from Battery industries.

Surface chemistry study

The type and net charge of functional groups bonded to the carbon surface is important in understanding the mechanism of adsorption of ionic adsorbates on activated carbons [10]. The adsorption capacity of activated carbon is influenced by functional groups on the carbon surface. The functional groups on the surface of activated carbon analyzed by the FTIR demonstrated the existence of carboxyl, hydroxyl, amine groups, amide groups, alkyl, aromatic C=C, Nitrile, Phenol and carboxylic groups (Table 6). The FTIR spectra of the carbonised and activated carbons showed some differences from each other. This demonstrates that after the activation, shifting occurred both to higher and lower wave numbers. This shifting indicated that there were binding processes taking place on the surfaces of the activated carbons during activation. FTIR spectra were obtained on a JASCO FTIR-3500 spectrometer. The analysis conditions used were 16 scans at a resolution of 4 cm^{-1} measured between 400 and 4000 cm^{-1}. The FTIR spectra of both carbonised (unactivated) and activated OBAC revealed complex surfaces as by the presence of several peaks observed (Table 6). The activated carbons showed more peaks than the carbonized Oil Bean shell. This is an indication that some reorganization of the surface oxides on subjection to chemical activation has taken place (Table 6). The peak observed around 1177 cm^{-1} for the carbonised OBAC shifted to around 1780 cm^{-1} in the activated OBAC. So also it was for the C=C aromatic bonding observed around 1574 cm^{-1} on the unactivated Oil Bean carbon shifted to 1750 cm^{-1}. The O-H stretch observed around 3223.80 cm^{-1} in the unactivated carbon and the C-H observed at 822.92 cm^{-1} also underwent various shifts as well. These results are similar to the ones reported for sawdust [11]. These functional groups could act as chemical binding agents where carboxyl, hydroxyl and amine groups could dissociate negatively charged active surface. This means that these functional groups could attract the positively charged objects such as heavy metal ions [12]. Looking at the FTIR spectra, it showed that chemical modification was very effective on chemical structure of activated carbon. Functional groups are formed during activation by interaction of free radicals on the carbon surface with atoms such as oxygen and nitrogen, both from within the precursor and from the atmosphere [13]. The functional groups render the surface of activated carbon chemically reactive and influence its adsorptive properties [14]. Surface oxidation is an inherent feature of activated carbon production. It results in hydroxyl (-OH), carbonyl (=CO), and carboxylic (-COOH) groups that impart an amphoteric character to the activated carbon. The FTIR spectra of both unactivated and the activated Snail Shell carbon also revealed complex surface going by the presence of several peaks (Table 7). The activated snail shell carbon showed more peaks than the unactivated snail shell carbon. This is an indication of the strong surface oxide reorganizations resulting from the interactions of the atoms of the activating agents (HCl, H_2SO_4 and H_3PO_4) used. There was shifting of observed peaks as well as disappearance of some observed peaks by the unactivated snail shell carbon prepared. The C=O of the aldehyde functional group was not observed in the unactivated carbon but was found in the activated SSAC. So also it was for C=C aromatic stretch. From Table 8, it can be deduced that carbonization at 600°C gave a better percentage adsorption compare to those of 800°C irrespective of the activating agents. In the adsorption of Cd by the OBAC, there was a better adsorption by those carbonized at 600°C since most of the percentages are higher than those of their counter parts excepts for some that were activated with HCl (Table 9).

In Table 10 Pb adsorbed better in OBAC carbonized at 800°C and as well had a high percentage of adsorption. This is shown pictorially by Figures 5-7. Just like Pb adsorption by OBAC, Mn was adsorbed better by those carbonized at 800°C even though the percentage adsorption was not that high (Table 11 and Figure 8). The AC carbonised at 800°C had a better percentage of adsorption except for those activated with H_3PO_4, but they all generally had a low percentage of adsorption (Table 12 and Figure 9).

Citation: Abugu HO, Okoye PAC, Ajiwe VIE, Omuku PE, Umeobika UC (2015) Preparation and Characterization of Activated Carbon Produced from Oil Bean (Ugba or Ukpaka) and Snail Shell. J Environ Anal Chem 2: 165. doi:10.4172/2380-2391.1000165

Oil Bean Shell Before Activation		After Activation	OBAC/600°C/HCl	OBAC/600°C/ H_3PO_4	OBAC/600°C/ H_2SO_4	OBAC/800°C/ HCl	OBAC/800°C/ H_3PO_4	OBAC/800°C/ H_2SO_4
Wave number	**Possible Assignments**	**Wave number**	**Possible Assignments**	**Possible Assignments**	**Possible Assignments**	**Possible Assignments**	**Possible Assignments**	**Possible Assignments**
822.92	Aromatic C – H stretching	860 – 680				Aromatic C – H Bending	Aromatic C – H Bending	Aromatic C – H Bending
958.1954		1780 – 1710	C=O Str. of COOH, Ketones, Esters	C=O Str. of COOH, Ketones, Esters	C=O Str. of COOH, Ketones, Esters.			
1177.18	Carboxylic acid C=0 stretch	1700 – 1500	Aromatic C=C Bending	Aromatic C=C Bending	Aromatic C=C Bending	Aromatic C=C Bending	Aromatic C=C Bending	Aromatic C=C Bending
1265.15		1680 – 1620	C=C Str. of Alkenes		C=C Str. of Alkenes	C=C Str. of Alkenes.		C=C Str. of Alkenes
1423.69		1690 – 1630	Amide, C=O Str.		Amide, C=O Str.	Amide, C=O Str.		Amide, C=O Str.
1574.504	Aromatic C=C bending	1750 – 1735	Aromatic C=H Bending	Aromatic C=H Bending	Aromatic C=H Bending	Aromatic C=H Bending	Aromatic C=H Bending	Aromatic C=H Bending
1806.151		1740 – 1690		Aldehyde C,=O Str.			Aldehyde C,=O Str.	
1882.47		1750 – 1680		Ketone C=O Str			Ketone C=O Str.	
2158.96	Alkyl C=C Stretch	2950 – 2850	C – H Str. of Alkanes	C – H Str. of Alkanes	C – H Str. of Alkanes	C – H Str. of Alkanes	C – H Str. of Alkanes	C – H Str. of Alkanes
2237.413	Nitrile C=N Strech	2260 – 2100	C=C Str. of Nitriles	C=C Str. of Nitriles	C=C Str. of Nitriles	C=C Str. of Nitriles	C=C Str. of Nitriles	C=C Str. of Nitriles
2905.61	Alkyl C-H Stretch							
3170.13	Alkyl C-H Stretch	3100 – 3010	C – H Str. of Aromatic ring				C – H Str. of Aromatic ring	C – H Str. of Aromatic ring
3223.80	Alcohol, phenol O - H stretch	3000 – 2500	O – H Str. of COOH, phenols, OH	O – H Str. of COOH, phenols, OH	O – H Str. of COOH, phenols, OH	O – H Str. of COOH, phenols, OH	O – H Str. of COOH, phenols, OH	O – H Str. of COOH, phenols, OH.
3351.445	Alcohol/phenol O-H stretch	3500 – 3300	N – H Str. of Amines			N – H Str. of Amines	N – H Str. of Amines	N – H Str. of Amines
3550.973	Amide N –H Stretch	3550 – 3200	OH O – H, Str.			OH O – H, Str.	OH O – H, Str.	OH O – H, Str.
3714.78	Amide N-H Stretch	3700 – 3500	Amide, N – H Str.			Amide, N – H Str.	Amide, N – H Str.	Amide, N – H Str.

Table 6: FTIR Analysis Oil Bean (In Nujol And Kbr As Solvents) (Source: Anirudhan et al.; Karthika et al.; Shen et al.; Bansal and Rao).

Snail Shell Before Activation		After Activation	SSAC/600°C/HCl	SSAC/600°C/ H_3PO_4	SSAC/600°C/ H_2SO_4	SSAC/800°C/ HCl	SSAC/800°C/ H_3PO_4	SSAC/800°C/ H_2SO_4
Wave number	**Possible Assignments**	**Wave number**	**Possible Assignments**	**Possible Assignments**	**Possible Assignments**	**Possible Assignments**	**Possible Assignments**	**Possible Assignments**
761.209		860 – 680	Aromatic C – H Bending	Aromatic C – H Bending	Aromatic C – H Bending	Aromatic C – H Bending	Aromatic C – H Bending	Aromatic C – H Bending
945.987		1780 – 1710	C=O Str. of COOH, Ketones, Esters					
1127.46		1700 – 1500	Aromatic C=C Bending	Aromatic C=C Bending				Aromatic C=C Bending
1495.913		1690 – 1630		Amide, C=O Str.	Amide, C=O Str.			Amide, C=O Str.
1751.494		1740 – 1690	Aldehyde C,=O Str.					
1987.339		2260 – 2220	C=C Str. of Nitriles	C=C Str. of Nitriles	C=C Str. of Nitriles		C=C Str. of Nitriles	
2544.37	Carboxylic Acid C –H Stretch	3300						
2873.69	Alkyl C –H Stretch							
3207.012	Amine N-H Stretch	3000 – 2500	O – H Str. of COOH, phenols, OH	O – H Str. of COOH, phenols, OH	O – H Str. of COOH, phenols, OH	O – H Str. of COOH, phenols, OH	O – H Str. of COOH, phenols, OH	O – H Str. of COOH, phenols, OH
3332.85	Amine N-H Stretch	3500 – 3300	N – H Str. of Amines	N – H Str. of Amines		N – H Str. of Amines	N – H Str. of Amines	N – H Str. of Amines
3474.62	Amine N-H Stretch	3550 – 3200	OH O – H, Str.	OH O – H, Str.	OH O – H, Str.	OH O – H, Str.	OH O – H, Str.	OH O – H, Str.
3614.68		3700 – 3500	Amide, N – H	Amide, N – H		Amide, N – H	Amide, N – H	

Table 7: FTIR Analysis Of Snail Shell (In Nujol And Kbr As Solvents) (Source: Anirudhan et al.; Karthika et al.; Shen et al.; Bansal and Rao).

HCl 600°C E (%)	HCl 800°C E (%)	H_2SO_4 600°C E (%)	H_2SO_4 800°C E (%)	H_3PO4 600°C E (%)	H_3PO4 800°C E (%)
97.5	87.8	96.8	43.4	84.3	59.7
96.8	90.1	94.7	41.9	81.0	60.7
90.3	89.9	88.2	42.7	82.7	63.9
8.99	38.2	94.6	41.1	82.0	19.7
42.7	4.9	60.9	54.2	32.0	11.1

OBAC=Oil Bean Activated Carbon

Table 8: Percentage Adsorption of Ni by OBAC.

HCl 600°C E%	HCl 800°C E%	H_2SO_4 600°C E%	H_2SO_4 800°C E%	H_3PO_4 600°C E%	H_3PO_4 800°C E%
71.7	63.3	98.9	39.9	58.4	30.5
61.6	78.6	97.6	29.9	55.6	24.8
60.3	77.7	99.1	27.6	59.2	23.8
17.9	36.4	96.9	9.2	18.0	4.9
7.04	6.96	71.3	3.4	14.8	12.3

Table 9: Percentage Adsorption of Cd by OBAC.

HCl 600°C E%	HCl 800°C E%	H_2SO_4 600°C E%	H_2SO_4 800°C E%	H_3PO_4 600°C E%	H_3PO_4 800°C E%
14.1	98.9	17.8	98.7	20.1	98.7
18.7	99.2	11.2	98.5	20.5	98.5
16.5	98.7	8.5	96.9	21.0	96.9
18.3	96.5	18.2	94.8	21.9	94.8
16.1	96.0	14.8	93.6	30.5	93.6

Table 10: Percentage Adsorption of Pb by OBAC.

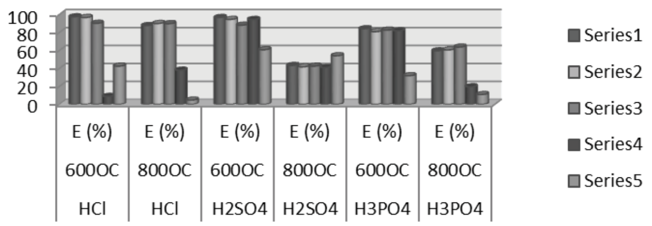

Figure 5: Percentage Adsorption of Ni by OBAC.

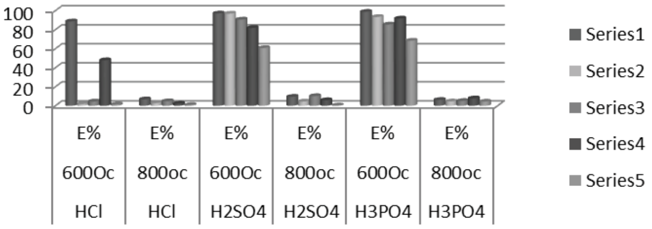

Figure 6: Percentage Adsorption of Cd by OBAC.

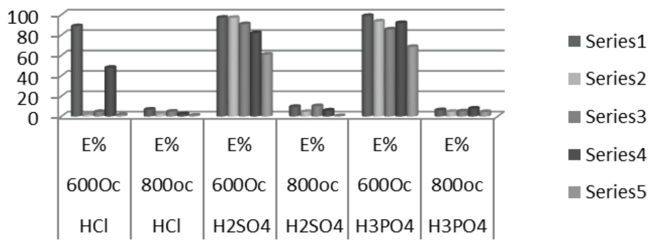

Figure 7: Percentage Adsorption of Pb by OBAC.

HCl 600°C E%	HCl 800°C E%	H_2SO_4 600°C E%	H_2SO_4 800°C E%	H_3PO_4 600°C E%	H_3PO_4 800°C E%
7.5	87.3	7.9	64.6	11.0	98.6
4.5	94.2	3.6	62.9	4.6	69.2
16.5	93.3	5.8	46.7	11.0	56.7
17.5	29.1	4.1	17.7	11.6	13.6
19.8	25.7	3.1	18.8	5.9	14.1

Table 11: Percentage Adsorption of Mn by OBAC.

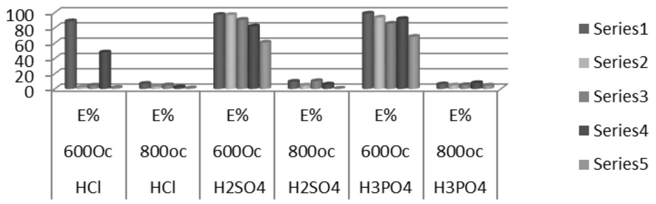

Figure 8: Percentage Adsorption of Mn by OBAC.

HCl 600°C E%	HCl 800°C E%	H_2SO_4 600°C E%	H_2SO_4 800°C E%	H_3PO_4 600°C E%	H_3PO_4 800°C E%
6.6	10.6	12.1	23.7	9.9	7.9
4.9	21.3	8.2	4.7	8.4	6.2
0.7	4.5	4.3	7.5	6.6	4.3
2.6	3..6	4.0	7.8	10.2	7.2
7.2	4.8	1.9	7.4	4.0	10.2

Table 12: Percentage Adsorption of Ni by SSAC.

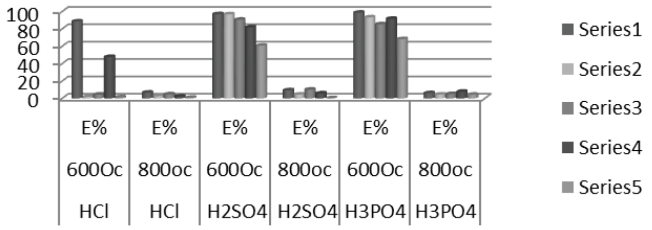

Figure 9: Percentage Adsorption of Ni by SSAC.

In the adsorption of Pb by SSAC, the AC carbonized at 600°C had a better percentage adsorption irrespective of the activating agent used though they all had low percentage of adsorption (Table 13 and Figure 10). The adsorption of Cd by SSAC carbonized at both temperature values and activated with different reagents/acids was very low in all though those carbonized at 600°C had a better percentage adsorption in most (Table 14 and Figure 11). The percentage adsorptions of Mn by SSAC were generally low though those carbonized at 600°C had a better adsorption especially those activated with H_3PO_4 and H_2SO_4 (Table 15 and Figure 12).

Quantitative description of sorption isotherm

Traditionally, the sorption of ions by adsorbents has been quantitatively described by parameters obtained either directly from isotherms or by least square analysis with Freundlich and Langmuir isotherms.

C	HCl 800°C E%	H_2SO_4 600°C E%	H_2SO_4 800°C E%	H_3PO_4 600°C E%	H_3PO_4 800°C E%
61.0	10.0	53.3	5.9	50.3	12.0
42.3	18.9	25.2	20.4	50.9	25.1
64.3	18.7	25.0	5.2	35.9	12.9
58.0	18.4	21.6	12.3	41.4	7.9
56.9	17.3	20.5	9.9	46.5	13.0

Table 13: Percentage Adsorption of Pb by SSAC.

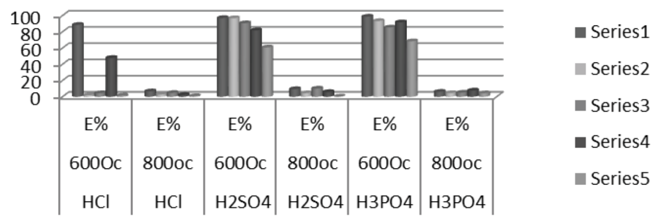

Figure 10: Percentage Adsorption of Pb by SSAC.

HCl 600°C E%	HCl 800°C E%	H_2SO_4 600°C E%	H_2SO_4 800°C E%	H_3PO_4 600°C E%	H_3PO_4 800°C E%
5.2	3.7	2.9	2.7	3.3	7.0
2.7	5.2	3.3	2.1	5.9	3.4
6.1	7.5	6.8	6.2	7.5	5.0
7.2	3.4	1.5	6.9	4.5	3.2
5.6	2.6	6.6	3.7	11.3	1.0

Table 14: Percentage Adsorption of Cd by SSAC.

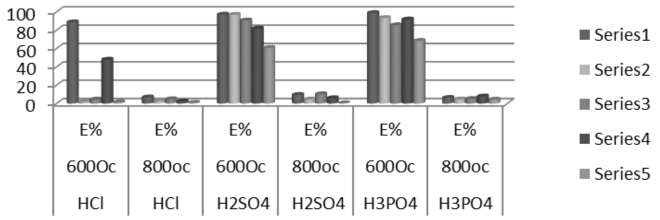

Figure 11: Percentage Adsorption of Cd by SSAC.

HCl 600°C E%	HCl 800°C E%	H_2SO_4 600°C E%	H_2SO_4 800°C E%	H_3PO_4 600°C E%	H_3PO_4 800°C E%
88.7	6.8	97.1	9.5	98.8	6.2
1.9	2.9	96.9	4.5	93.4	4.6
4.5	4.8	90.7	10.2	85.5	5.1
47.9	2.3	81.9	5.9	91.8	7.8
1.47	0.9	60.8	0.4	68.4	4.4

Table 15: Percentage Adsorption of Mn by SSAC.

The data from this study was subjected to Freundlich and Langmuir models to determine sorption parameters and identify the model which best fit or describes the adsorption by these prepared activated carbons.

The Freundlich model is a case for heterogeneous surface energies and it gives an exponential distribution of active sites present in the activated carbon (AC). This form of the equation was used to relate the amount of heavy metal ions sorbed from the metal solutions and the linear form of the model is:

$$\log q_e = \log K_f + 1/n \log Ce$$

Where q_e is the amount of sorbed metal ions in mg/g, Ce is the equilibrium concentration of the metal ions. n and K_f are the Freundlich constants which respectively indicates the adsorption intensity and the adsorption capacity of the AC [15]. They are calculated from the slope and intercept of the plot of logq$_e$ versus log Ce (Table 16).

The Freundlich adsorption intensity (n) for the OBAC carbonised at 600°C ranged from 1.14 to 15.6 (Table 64). The higher the value of n, the stronger bond between the adsorbent and the adsorbate, a desired parameter in waste water treatment [16] n is >1 for Ni adsorption on each OBAC (Table 64). A similar result was obtained for coconut shell carbon adsorption of Methylene Blue [17]. Figure 3 shows the result of the adsorption isotherm for Ni on OBAC carbonised at 600°C and activated with HCl. From the figure, the straight line plot indicates the occurrence of Ni metal adsorption from the sample. The graph shows the adsorption isotherm is of relative good Ni removal. This can be proved by looking at the coefficient of determination, R^2=0.603. The Goodness of fit of an experimental data is measured by the determination coefficient (R^2) [18]. The R^2 for all the isotherms are presented in Table 64. The slope of the linear plot is also good and suitable for testing the adsorption effectiveness. The value of n obtained from the slope of the linear plot ranged from 1.91 to 15.9 which indicate the strength of the OBAC as an adsorbent. When n>1, the adsorption coefficient increases with increasing concentration of the solution which lead to an increase in hydrophobic surface characteristic after monolapisan and when n<1, K_f decreases with concentration [19]. Appendix 4 shows the Atomic Absorption Spectrophotometer (AAS) results of the heavy metal analysis (Figure 13). The Langmuir isotherm model suggests that sorption occurs on homogeneous surface by monolayer sorption

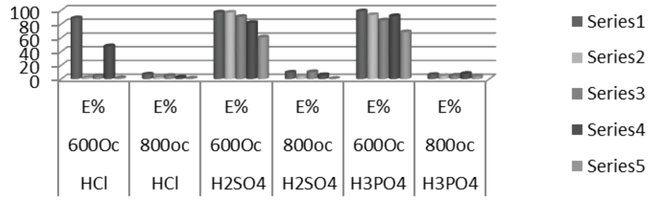

Figure 12: Percentage Adsorption of Mn by SSAC.

C_o(mg/l)	C_e (mg/l)	q_e (mg/g)	E (%)	$\log q_e$	$\log C_e$	$1/q_e$	$1/C_e$
55.472	1.39	0.54	97.5	-0.268	0.143	1.852	0.7194
52.672	1.67	0.51	96.8	-0.292	0.204	1.961	0.5988
59.352	5.73	0.54	90.3	-0.268	0.758	1.852	0.1745
64.965	6.58	0.58	8.99	-0.237	0.818	1.724	0.1520
66.797	38.26	0.29	42.7	-0.538	1.583	3.448	0.0261

C_o=initial metal concentration, $C_{e=}$equilibrium metal concentration, $q_{e=}$metal adsorbed per gram activated carbon and E=Percentage adsorption efficiency.

Table 16: Ni Adsorption by Oil Bean Carbonized at 600°C and Activated with HCl.

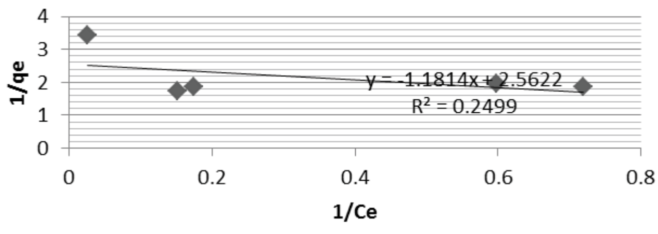

Figure 13: Freundlich isotherm plot for Ni onto OBAC Carbonized at 600°C and activated with HCl.

without interaction between sorbed ions. The linear form of Langmuir isotherm equation is as presented below:

$1/qe=1/Q^o+1/bQ^o 1/Ce$

Where Ce is the equilibrium concentration (mg/l), q_e is the amount of metal ions adsorbed at equilibrium (mg/g) and the Q^o and b are the Langmuir isotherm constants which gives the adsorption capacity and the energy of adsorption respectively [14]. The linear plot of $1/q_e$ versus 1/Ce indicates the Langmuir model plot and the values of Q^o and b were calculated from the slopes and intercepts of the Langmuir plots. In Figure 3, the determination coefficient did not show a good fit. The Langmuir adsorption capacity (Q^o) of the three type of OBAC for Ni ranged from 0.035 to 1.4144 l/kg while the Langmuir energy of adsorption (b) ranged from 0.32 to 5.895 which reflect the retention intensity and the number of sites available for a sorbate (Figure 14 and Table 17). Figure 3 indicates a good determination coefficient (0.693). Also, the adsorption intensity was relatively high (12.9) as well as a good adsorption capacity of 1.8 (Figures 15, 16 and Tables 18, 19). For the adsorption of Ni by OBAC carbonised at 800°C, the K_f ranged from 2.5 to 2.9 which is an indication of good adsorptive capacity. Also, the adsorption intensity ranged from 0.001 to 0.739. The determination coefficient of the Freundlich plot indicates poor fit except for that activated with HCl. The adsorption data for OBAC carbonised at 600°C had a better fit for the Freundlich model. The Freundlich intensity of adsorption (n) of Ni on OBAC was relatively high, but the reverse was the case for the Freundlich adsorption capacity of the (K_f) values OBAC. The Langmuir isotherm for Ni adsorption onto OBAC carbonised at 800°C showed a poor fit considering the determination coefficient (R^2) for the plot of the experimental data obtained for adsorption of Ni on OBAC. Their adsorption capacities ranged from 0.0035 to 0.012 while the energy of adsorption ranged from 0.8 to 17.7 (Tables 20-22). Considering the values of the determination coefficients of the Freundlich model, the adsorption of Cd by OBAC carbonised at 600°C had a better fit (0.917, 0.739, 0.999 for HCl, H_2SO_4, H_3PO_4 activating agents respectively) though they all had a relatively good fit values except for that activated with H_2SO_4 (R^2=0.022). In terms of the adsorption intensity, those carbonised at 800°C were better than their counterparts, but the reverse was the case with the adsorption capacity (K_f) (Tables 23-25). The Langmuir adsorption isotherm plot of the adsorption of Cd on OBAC carbonized at 600°C and 800°C had low R^2 values. This indicates a poor fit of the experimental data generated. The R^2 values ranged from 0.348 to 0.993. This is in exception of those Oil Bean carbon activated with H_2SO_4 at both temperatures of carbonization. Despite the poor fit of the experimental data on the Langmuir isotherm model, the Q^o values were also very low and that indicates the low adsorption capacity of Cd on the carbon types prepared. The Langmuir adsorption energy term was relatively high (Tables 26, 27). Generally, in the OBAC adsorption of Cd, OBAC activated with H_2SO_4 had higher Freundlich adsorption intensity (n=1.14, 1.75 at 600°C and 800°C respectively) in both carbonization temperatures, but in their Freundlich adsorption capacities (K_f), the ones activated with H_3PO_4 (43.1, 7.6×10^5 at 600°C and 800°C respectively) were better and the least was recorded by those activated with H_2SO_4 (Tables 27, 28). The adsorption of Cd by OBAC carbonized at different temperature and activated with different acids as activating agent, had a good fit for the Freundlich Isotherm Model considering their respective determination coefficients, though those carbonized at 800°C had a better fit in the case of the three activating agents excepts for the 800°C/H_3PO_4 OBAC, which was low (R^2=0.089). Also, those carbonized at 800°C had a better adsorption intensity (n=4.46, 29.4, 4.63 for HCl, H_3PO_4 and H_2SO_4 respectively), than those carbonized at 600°C irrespective of their activating agents. For their respective Freundlich adsorption capacity (K_f), those carbonized at 600°C were better than their counterparts except for that activated with H_2SO_4 (Tables 29, 30). The experimental data for the adsorption of Pb on OBAC had a good fit on the Langmuir isotherm model having had the determination coefficient ranging from 0.004 to 0.9950. This is in exception of that activated with H_2SO_4 at both 600°C and 800°C carbonization temperature and that activated with H_3PO_4 at 600°C. It also had low Q^o values as well as low b values indicating poor Langmuir adsorption capacity and adsorption energy (Tables 31-34). The determination coefficients for the adsorption of Mn by OBAC where generally low and so the Freundlich isotherm plot did not fit well except for that carbonized at 800°C and activated with HCl (R^2=0.826). The metal adsorption intensity as well as the Freundlich adsorption capacities were all relatively high, though those carbonized at 800°C where better than their counterparts, except for that activated with HCl at 600°C, which was very high in its adsorption capacity (K_f=4.9×10^5) (Tables 35, 36). For Mn adsorption on OBAC, the experimental data generated did not have a good fit on Langmuir isotherm model in all the types of activated carbon produced except for that activated with HCl and carbonized at 800°C (R^2=0.892). The R^2 ranged from 0.008 to 0.892. The Langmuir adsorption energy (b) was relatively high while the Langmuir adsorption capacity constant (Q^o) was low (Table 37-40). The determination coefficient from Ni adsorption on SSAC carbonized at 600°C and 800°C were all low and indicates a poor fit of the adsorption data on Freundlich isotherm model. R^2 ranged from 0.57 to 0.927. It was only that carbonized at 600°C and activated with H_2SO_4 and that carbonized at 800°C and activated with HCl that had a good fit (R^2=0.710 and 0.927 respectively). The Freundlich adsorption capacity constants were very high indicating a good adsorption capacity of the SSAC. So also it was for the Freundlich adsorption intensities which ranged from 0.23 to 1.07 (Tables 41-43). The adsorption data for Ni on SSAC had a poor fit on the Langmuir isotherm model as the coefficient of determination ranges from 0.029 to 0.800. The Q^o were very low but the reverse was the case for the Langmuir adsorption energy constant (Tables 44-46).

The Freundlich model did not fit well with the adsorption data of the SSAC for Pb, taking a look at the determination coefficient values recorded, which ranges from 0.031 to 0.555, but the n and K_f values were relatively high indicating good adsorption intensities and adsorption capacities (Tables 47-49). The Langmuir plot for adsorption of Pb on SSAC followed the same pattern just like the adsorption of Ni by SSAC. The R^2 values were low and the range is from 0.029 to 0.451. Also, the Q^o which is the Langmuir adsorption capacity constant were low. It ranged from 0.00013 to 0.061. The Langmuir adsorption energy constant (b) ranged from 5.1 to 120.9 indicating good adsorption energy for the adsorption of Pb on SSAC (Tables 50-52). The adsorption data of Cd on SSAC were also very poorly fitted on the Freundlich model as the determination coefficient (R^2) ranged from 0.001 to 0.890. The adsorption intensity parameter was also low (0.11 to 1.33). Unlike the adsorption intensity term, the adsorption capacity term were very high and so indicates the poor fit nature of the isotherm plot (Tables 53-58). The adsorption of Mn on SSAC data were also very poorly fitted on the Freundlich model since the determination coefficient (R^2) ranged from 0.099 to 0.563. The n and the K_f values are relatively high indicating a high adsorption capacity as well. They ranged from 0.82 to 19.61 and 1.1 to 586.1 respectively (Tables 59, 60). The adsorption of Cd and Mn by SSAC experimental data fitted poorly on the Langmuir isotherm model plot. Their respective R^2 ranges from 0.002 to 0.852 and 0.152 to 0.813. the adsorption energy constant were relatively high for both, but the Q^o values were very low indicating low adsorption capacity of SSAC prepared from snail shell (Tables 61-63). Freundlich isotherm

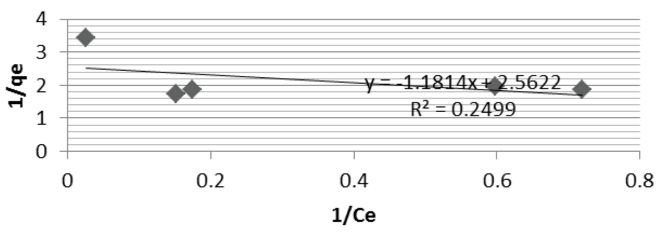

Figure 14: Langmuir isotherm plot for Ni onto OBAC Carbonized at 600°C and activated with HCl.

C_o(mg/l)	C_e (mg/l)	q_e (mg/g)	E (%)	$\log q_e$	$\log C_e$	$1/q_e$	$1/C_e$
55.472	1.78	0.54	96.8	-0.268	0.250	1.8519	0.5618
52.672	2.77	0.50	94.7	-0.301	0.442	2.0000	0.3610
59.352	6.98	0.52	88.2	-0.284	0.844	1.9231	0.1433
64.965	16.50	0.48	94.6	-0.319	1.217	2.0833	0.0606
66.797	26.10	0.41	60.9	-0.387	1.417	2.4390	0.0383

Table 17: Ni Adsorption by Oil Bean Carbonized at 600°C and Activated with H_2SO_4.

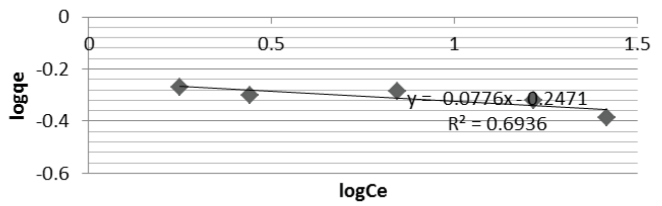

Figure 15: Freundlich isotherm plot for Ni onto OBAC Carbonized at 600°C and activated with H_2SO_4.

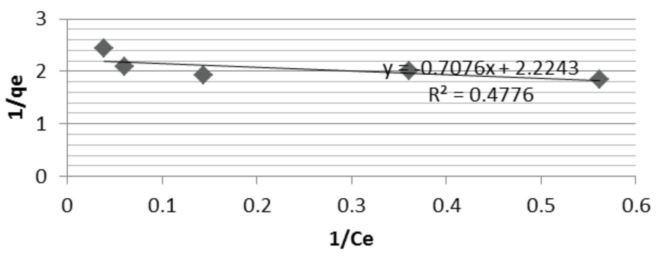

Figure 16: Langmuir isotherm plot for Ni onto OBAC Carbonized at 600°C and activated with H_2SO_4.

model as earlier mentioned is a case for heterogeneous surface energies and it gives an exponential distribution of active sites. The Freundlich constants n and K_f which respectively indicates the adsorption intensity and adsorption capacity were calculated from the slope and intercept of the plot of $\log q_e$ versus $\log C_e$ which have been presented in the previous pages and the parameters summarized in Table 64. The Freundlich binding capacities for Activated carbon produced from Oil Bean ranged from 1.0 to 7.6 × 10^5 (Table 64). The increasing value indicates greater adsorption capacity. The value of n is a function of the strength of the adsorbent materials used and it gives an indication of the favourability of adsorption. As n>1, favourable adsorption condition is observed. When the value of n is high, it showed the adsorption bond is weak and when n>1, the absorption coefficient increases with increasing concentration of the solution which lead to an increase in the surface characteristic after monolayer adsorption. When the value of n<1 K_f decreased with concentration in most of the activated carbon types. This is in line with previous studies [19]. The goodness of fit of an experimental data is measured by the determination coefficients or data realiability (R^2) Zaid and Mohammed [18]. The R^2 for the isotherm studied as summarized in Table 64 and it could be deduced that the Freundlich model showed a good fit for all the Oil Bean activated carbon except for Cd/OBAC/800°C H_3PO_4, Mn/OBAC/600°C/H_2SO_4, Ni/OBAC/800°C/H_2SO_4, Pb/OBAC/800°C/H_2SO_4 and Mn/OBAC/600°C/H_3PO_4. Table 65 shows the Freundlich adsorption isotherm parameters for the adsorption of Ni, Pb, Cd and Mn by the activated carbons produced from Snail shell. The Freundlich model fitted very poorly virtually in all the types of activated carbons under consideration. This in turn affected the values of their respective adsorption intensities as well as their adsorption capacities (Table 65). The Langmuir isotherm

C_o(mg/l)	C_e (mg/l)	q_e (mg/g)	E (%)	$\log q_e$	$\log C_e$	$1/q_e$	$1/C_e$
55.472	8.67	0.47	84.3	-0.328	0.938	2.128	0.1153
52.672	9.98	0.43	81.0	-0.366	0.999	2.326	0.1002
59.352	10.26	0.49	82.7	-0.310	1.011	2.041	0.0975
64.965	11.66	0.53	82.0	-0.276	1.067	1.887	0.0858
66.797	45.36	0.21	32.0	-0.678	1.657	4.762	0.0220

Table 18: Ni Adsorption by Oil Bean Carbonized at 600°C and Activated with H_3PO_4.

C_o(mg/l)	C_e (mg/l)	q_e (mg/g)	E (%)	$\log q_e$	$\log C_e$	$1/q_e$	$1/C_e$
55.472	6.78	0.49	87.8	-0.310	0.831	2.0408	0.1475
52.672	5.19	0.47	90.1	-0.328	0.715	2.1277	0.0157
59.352	6.003	0.53	89.9	-0.276	0.778	1.8868	0.1666
64.965	40.13	0.25	38.2	-0.602	1.603	4.0000	0.0249
66.797	63.53	0.03	4.9	-1.523	1.803	33.333	0.0157

Table 19: Ni Adsorption by Oil Bean Carbonized at 800°C and Activated with HCl.

C_o(mg/l)	C_e (mg/l)	q_e (mg/g)	E (%)	$\log q_e$	$\log C_e$	$1/q_e$	$1/C_e$
55.472	31.38	0.24	43.4	-0.620	1.497	4.1667	0.0319
52.672	30.56	0.22	41.9	-0.658	1.485	4.5455	0.0327
59.352	34.01	0.25	42.7	-0.602	1.532	4.0000	0.0294
64.965	38.27	0.27	41.1	-0.569	1.583	3.7037	0.0261
66.797	30.60	0.36	54.2	-0.444	1.486	2.7778	0.0327

Table 20: Ni Adsorption by Oil Bean carbonized at 800°C and Activated with H_2SO_4.

C_o(mg/l)	C_e (mg/l)	q_e (mg/g)	E (%)	$\log q_e$	$\log C_e$	$1/q_e$	$1/C_e$
55.472	22.37	0.33	59.7	-0.481	1.350	3.030	0.04470
52.672	20.68	0.32	60.7	-0.495	1.316	3.025	0.0484
59.352	21.38	0.38	63.9	-0.420	1.330	2.632	0.0468
64.965	52.17	0.13	19.7	-0.886	1.717	7.692	0.0192
66.797	59.38	0.07	11.1	-1.155	1.774	14.286	0.0168

Table 21: Ni Adsorption by Oil Bean Carbonized at 800°C and Activated with H_3PO_4.

C_o(mg/l)	C_e (mg/l)	q_e (mg/g)	E (%)	$\log q_e$	$\log C_e$	$1/q_e$	$1/C_e$
53.662	15.19	0.38	71.7	-0.420	1.182	2.6316	0.0658
53.057	20.37	0.33	61.6	-0.481	1.309	3.0303	0.0491
53.930	21.38	0.33	60.3	-0.481	1.330	3.0303	0.0468
55.728	45.74	0.10	17.9	-1.000	1.660	10.0000	0.0219
57.470	53.426	0.04	7.04	-1.398	1.728	25.0000	0.0187

Table 22: Cd Adsorption by Oil Bean Carbonized at 600°C and Activated with HCl.

C_o(mg/l)	C_e (mg/l)	q_e (mg/g)	E (%)	$\log q_e$	$\log C_e$	$1/q_e$	$1/C_e$
53.662	0.57	0.53	98.9	-0.276	-0.244	1.8868	1.7544
53.057	1.28	0.52	97.6	-0.284	0.107	1.9231	0.7813
53.930	0.51	0.53	99.1	-0.276	-0.292	1.8868	1.9608
55.728	1.681	0.54	96.9	-0.268	0.226	1.8519	0.5949
57.470	16.47	0.41	71.3	-0.387	1.217	2.4390	0.0607

Table 23: Cd Adsorption by Oil Bean Carbonized at 600°C and Activated with H_2SO_4.

C_o(mg/l)	C_e (mg/l)	q_e (mg/g)	E (%)	$\log q_e$	$\log C_e$	$1/q_e$	$1/C_e$
53.662	22.33	0.31	58.4	-0.509	1.349	3.2258	0.0448
53.057	23.56	0.29	55.6	-0.538	1.372	3.4483	0.0424
53.930	21.99	0.32	59.2	-0.495	1.342	3.1250	0.0455
55.728	45.67	0.10	18.0	-1.000	1.660	10.0000	0.0219
57.470	48.96	0.09	14.8	-1.046	1.690	11.1111	0.0204

Table 24: Cd Adsorption by Oil Bean Carbonized at 600°C and Activated with H_3PO_4.

C_o(mg/l)	C_e (mg/l)	q_e (mg/g)	E (%)	$\log q_e$	$\log C_e$	$1/q_e$	$1/C_e$
53.662	19.69	0.34	63.3	-0.469	1.294	2.9412	0.0508
53.057	11.38	0.42	78.6	-0.377	1.056	2.3810	0.0879
53.930	12.022	0.42	77.7	-0.377	1.080	2.3810	0.0832
55.728	35.452	0.20	36.4	-0.699	1.550	5.0000	0.0282
57.470	53.407	0.04	6.96	-1.398	1.728	25.0000	0.0187

Table 25: Cd Adsorption by Oil Bean Carbonized at 800°C and Activated with HCl.

C_o(mg/l)	C_e (mg/l)	q_e (mg/g)	E (%)	$\log q_e$	$\log C_e$	$1/q_e$	$1/C_e$
53.662	37.28	0.16	30.5	-0.796	1.571	6.2500	0.0268
53.057	39.90	0.13	24.8	-0.886	1.601	7.6923	0.0251
53.930	42.10	0.12	23.8	-0.921	1.624	8.3333	0.0238
55.728	53.00	0.27	4.9	-0.569	1.724	3.7037	0.0189
57.470	52.18	0.05	12.3	-1.301	1.718	20.0000	0.0192

Table 26: Cd Adsorption by Oil Bean Carbonized at 800°C and Activated with H_3PO_4.

C_o(mg/l)	C_e (mg/l)	q_e (mg/g)	E (%)	$\log q_e$	$\log C_e$	$1/q_e$	$1/C_e$
53.662	32.33	0.21	39.9	-0.678	1.510	4.7619	0.0309
53.057	37.16	0.16	29.9	-0.796	1.570	6.2500	0.0269
53.930	39.04	0.15	27.6	-0.824	1.592	6.6667	0.0256
55.728	50.59	0.05	9.2	-1.301	1.704	20.0000	0.0198
57.470	55.49	0.02	3.4	-1.699	1.744	50.0000	0.0180

Table 27: Cd Adsorption by Oil Bean Carbonized at 800°C and Activated with H_2SO_4.

C_o(mg/l)	C_e (mg/l)	q_e (mg/g)	E (%)	$\log q_e$	$\log C_e$	$1/q_e$	$1/C_e$
35.724	30.68	0.05	14.1	-1.301	1.487	20.0000	0.0326
37.606	30.56	0.07	18.7	-1.155	1.485	14.2857	0.0327
43.912	36.66	0.07	16.5	-1.155	1.564	14.2857	0.0273
57.167	46.72	0.10	18.3	-1.000	1.670	10.0000	0.0214
57.381	48.14	0.09	16.1	-1.046	1.683	11.1111	0.0208

Table 28: Pb Adsorption by Oil Bean Carbonized at 600°C and Activated with HCl.

C_o(mg/l)	C_e (mg/l)	q_e (mg/g)	E (%)	$\log q_e$	$\log C_e$	$1/q_e$	$1/C_e$
35.724	28.55	0.07	20.1	-1.1549	1.4556	14.2857	0.0350
37.606	29.91	0.08	20.5	-1.0969	1.4758	12.5000	0.0334
43.912	34.71	0.09	21.0	-1.0458	1.5405	1.1111	0.0288
57.167	44.66	0.13	21.9	-0.8861	1.6499	7.6923	0.0224
57.381	39.87	0.18	30.5	-0.7447	1.6006	5.5556	0.0251

Table 29: Pb Adsorption by Oil Bean Carbonized at 600°C and Activated with H_3PO_4.

C_o(mg/l)	C_e (mg/l)	q_e (mg/g)	E (%)	$\log q_e$	$\log C_e$	$1/q_e$	$1/C_e$
35.724	29.36	0.06	17.8	-1.222	1.468	16.6667	0.0341
37.606	33.40	0.04	11.2	-1.398	1.524	25.0000	0.0299
43.912	40.16	0.04	8.5	-1.398	1.604	25.0000	0.0249
57.167	46.76	0.10	18.2	-1.000	1.670	10.0000	0.0214
57.381	48.88	0.09	14.8	-1.046	1.689	11.1111	0.0205

Table 30: Pb Adsorption by Oil Bean Carbonized at 600°C and Activated with H_2SO_4.

C_o(mg/l)	C_e (mg/l)	q_e (mg/g)	E (%)	$\log q_e$	$\log C_e$	$1/q_e$	$1/C_e$
35.724	0.41	0.35	98.9	-0.4559	-0.3872	2.8571	2.4390
37.606	0.31	0.37	99.2	-0.4318	-0.5086	2.7027	3.2258
43.912	0.57	0.43	98.7	-0.3665	-0.2441	2.3256	1.7544
57.167	1.98	0.55	96.5	-0.2596	0.2967	1.8182	0.5051
57.381	2.31	0.55	96.0	-0.2596	0.3636	1.8182	0.4329

Table 31: Pb Adsorption by Oil Bean Carbonized at 800°C and Activated with HCl.

C_o(mg/l)	C_e (mg/l)	q_e (mg/g)	E (%)	$\log q_e$	$\log C_e$	$1/q_e$	$1/C_e$
35.724	0.48	0.35	98.7	-0.4559	-0.3188	2.8571	2.08333
37.606	0.55	0.37	98.5	-0.4318	-0.2596	2.7027	1.8182
43.912	1.38	0.43	96.9	-0.3665	0.1399	2.3256	0.7246
57.167	2.99	0.54	94.8	-0.2676	0.4757	1.8519	0.3344
57.381	3.67	0.54	93.6	-0.2676	0.5647	1.8519	0.2725

Table 32: Pb Adsorption by Oil Bean Carbonized at 800°C and Activated with H_3PO_4.

C_o(mg/l)	C_e (mg/l)	q_e (mg/g)	E (%)	$\log q_e$	$\log C_e$	$1/q_e$	$1/C_e$
35.724	0.54	0.35	98.5	-0.4559	-0.2676	2.8571	1.8519
37.606	0.07	0.38	99.8	-0.4202	-1.1549	2.6316	14.2857
43.912	0.01	0.44	99.9	-0.3565	-2.0000	2.2727	100.0000
57.167	0.30	0.57	99.5	-0.2441	-0.5288	1.7544	3.3333
57.381	1.37	0.56	97.6	-0.2518	0.1367	1.7857	0.7299

Table 33: Pb Adsorption by Oil Bean Carbonized at 800°C and Activated with H_2SO_4.

C_o (mg/l)	C_e (mg/l)	q_e (mg/g)	E (%)	$\log q_e$	$\log C_e$	$1/q_e$	$1/C_e$
75.046	69.42	0.06	7.5	-1.2218	1.8415	16.6667	0.0144
114.686	109.55	0.05	4.5	-1.3010	2.0396	20.0000	0.0091
135.240	112.86	0.22	16.5	-0.6576	2.0525	4.5455	0.0089
145.137	120.14	0.25	17.5	-0.6021	2.0797	4.0000	0.0083
147.280	118.11	0.29	19.8	-0.5376	2.0723	3.4483	0.0085

Table 34: Mn Adsorption by Oil Bean Carbonized at 600°C and Activated with HCl.

C_o (mg/l)	C_e (mg/l)	q_e (mg/g)	E (%)	$\log q_e$	$\log C_e$	$1/q_e$	$1/C_e$
75.046	66.81	0.08	11.0	-1.0969	1.8248	12.5000	0.0149
114.686	109.40	0.05	4.6	-1.3010	2.0390	20.0000	0.0091
135.240	120.30	0.15	11.0	-0.8239	2.0803	6.6667	0.0083
145.137	128.34	0.17	11.6	-0.7695	2.1084	5.8824	0.0078
147.280	138.56	0.09	5.9	-1.0458	2.1416	11.1111	0.0072

Table 35: Mn Adsorption by Oil Bean Carbonized at 600°C and Activated with H_3PO_4.

C_o (mg/l)	C_e (mg/l)	q_e (mg/g)	E (%)	$\log q_e$	$\log C_e$	$1/q_e$	$1/C_e$
75.046	69.12	0.06	7.9	-1.2218	1.8396	16.6667	0.0145
114.686	110.56	0.04	3.6	-1.3979	2.0436	25.0000	0.0090
135.240	127.40	0.07	5.8	-1.1549	2.1052	14.2857	0.0078
145.137	139.20	0.06	4.1	-1.2218	2.1436	16.6667	0.0072
147.280	142.70	0.05	3.1	-1.3010	2.1544	20.0000	0.0070

Table 36: Mn Adsorption by Oil Bean Carbonized at 600°C and Activated with H_2SO_4.

C_o(mg/l)	C_e (mg/l)	q_e (mg/g)	E (%)	$\log q_e$	$\log C_e$	$1/q_e$	$1/C_e$
75.046	9.51	0.66	87.3	-0.1805	0.9782	1.5151	0.1052
114.686	6.66	1.08	94.2	0.0334	0.8235	0.9259	0.1502
135.240	9.011	1.26	93.3	0.1004	0.9548	0.7937	0.1110
145.137	102.9	0.42	29.1	-0.3768	2.0124	2.3810	0.0097
147.280	109.5	0.38	25.7	-0.4202	2.0394	2.6316	0.0091

Table 37: Mn Adsorption by Oil Bean Carbonized at 800°C and Activated with HCl.

C_o (mg/l)	C_e (mg/l)	q_e (mg/g)	E (%)	$\log q_e$	$\log C_e$	$1/q_e$	$1/C_e$
75.046	1.06	0.74	98.6	-0.1308	0.0253	1.3514	0.9434
114.686	35.28	0.79	69.2	-0.1024	1.5475	1.2658	0.0283
135.240	58.53	0.77	56.7	-0.1135	1.7674	1.2987	0.0171
145.137	125.43	0.20	13.6	-0.6990	2.0984	5.0000	0.0080
147.280	126.59	0.21	14.1	-0.6778	2.1024	4.7619	0.0079

Table 38: Mn Adsorption by Oil Bean Carbonized at 800°C and Activated with H_3PO_4.

C_o(mg/l)	C_e (mg/l)	q_e (mg/g)	E (%)	$\log q_e$	$\log C_e$	$1/q_e$	$1/C_e$
75.046	26.57	0.48	64.6	-0.3188	1.4244	2.0833	0.0376
114.686	42.53	0.72	62.9	-0.1427	1.6287	1.3889	0.0235
135.240	72.12	0.63	46.7	-0.2007	1.8581	1.5873	0.0139
145.137	119.48	0.26	17.7	-0.5850	2.0773	3.8462	0.0084
147.280	119.55	0.28	18.8	-0.5528	2.0775	3.5714	0.0084

Table 39: Mn Adsorption by Oil Bean Carbonized at 800°C and Activated with H_2SO_4.

C_o(mg/l)	C_e (mg/l)	q_e (mg/g)	E (%)	$\log q_e$	$\log C_e$	$1/q_e$	$1/C_e$
55.47	51.8	0.04	6.6	-1.3979	1.7143	25.0000	0.0193
52.67	50.11	0.03	4.9	-1.5229	1.6999	33.3333	0.0200
59.35	58.96	0.01	0.7	-2.0000	1.7706	100.0000	0.0170
64.97	63.28	0.02	2.6	-1.6990	1.8013	50.0000	0.0158
66.79	61.99	0.05	7.2	-1.3010	1.7923	20.0000	0.0161

Table 40: Ni Adsorption by Snail shell Carbonized at 600°C and Activated with HCl.

C_o(mg/l)	C_e (mg/l)	q_e (mg/g)	E (%)	$\log q_e$	$\log C_e$	$1/q_e$	$1/C_e$
55.47	49.96	0.06	9.9	-1.2218	1.6986	16.6667	0.0200
52.67	48.23	0.04	8.4	-1.3979	1.6833	25.0000	0.0128
59.35	55.42	0.04	6.6	-1.3979	1.7437	25.0000	0.0180
64.97	58.36	0.07	10.2	-1.1549	1.7661	14.2857	0.0172
66.79	64.12	0.03	4.0	-1.5259	1.8070	33.3333	0.0156

Table 41: Ni Adsorption by Snail shell Carbonized at 600°C and Activated with H_3PO_4.

C_o(mxg/l)	C_e (mg/l)	q_e (mg/g)	E (%)	$\log q_e$	$\log C_e$	$1/q_e$	$1/C_e$
55.47	48.78	0.07	12.1	-1.1549	1.6882	14.2857	0.0205
52.67	48.37	0.04	8.2	-1.3979	1.6846	25.0000	0.0207
59.35	56.79	0.03	4.3	-1.5229	1.7543	33.3333	0.0176
64.97	62.38	0.03	4.0	-1.5229	1.7950	33.3333	0.0160
66.79	65.49	0.01	1.9	-2.0000	1.8162	100.0000	0.0153

Table 42: Ni Adsorption by Snail shell Carbonized at 600°C and Activated with H_2SO_4.

C_o(mg/l)	C_e (mg/l)	q_e (mg/g)	E (%)	$\log q_e$	$\log C_e$	$1/q_e$	$1/C_e$
55.47	49.6	0.06	10.6	-1.2218	1.6955	16.6667	0.0202
52.67	41.46	0.11	21.3	-0.9586	1.6176	9.0909	0.0241
59.35	56.70	0.03	4.5	-1.5229	1.7536	33.3333	0.0176
64.97	62.66	0.02	3..6	-1.6990	1.7970	50.0000	0.0160
66.79	63.57	0.03	4.8	-1.5229	1.8033	33.3333	0.0157

Table 43: Ni Adsorption by Snail shell Carbonized at 800°C and Activated with HCl.

C_o(mg/l)	C_e (mg/l)	q_e (mg/g)	E (%)	$\log q_e$	$\log C_e$	$1/q_e$	$1/C_e$
55.47	51.09	0.04	7.9	-1.3979	1.7083	25.0000	0.0196
52.67	49.38	0.03	6.2	-1.5229	1.6936	33.3333	0.0202
59.35	56.78	0.03	4.3	-1.5229	1.7542	33.3333	0.0176
64.97	60.29	0.05	7.2	-1.3010	1.7802	20.0000	0.0166
66.79	59.96	0.07	10.2	-1.1549	1.7779	14.2857	0.0167

Table 44: Ni Adsorption by Snail shell Carbonized at 800°C and Activated with H_3PO_4.

C_o(mg/l)	C_e (mg/l)	q_e (mg/g)	E (%)	$\log q_e$	$\log C_e$	$1/q_e$	$1/C_e$
55.47	42.32	0.13	23.7	-0.8861	1.6265	7.6923	0.0236
52.67	50.19	0.02	4.7	-1.6990	1.7006	50.0000	0.0199
59.35	54.89	0.04	7.5	-1.3979	1.7395	25.0000	0.0182
64.97	59.91	0.05	7.8	-1.3010	1.7775	20.0000	0.0167
66.79	61.88	0.05	7.4	-1.3010	1.7916	20.0000	0.0162

Table 45: Ni Adsorption by Snail shell Carbonized at 800°C and Activated with H_2SO_4.

C_o(mg/l)	C_e (mg/l)	q_e (mg/g)	E (%)	$\log q_e$	$\log C_e$	$1/q_e$	$1/C_e$
35.70	13.89	0.52	61.0	-0.6576	1.1427	4.5455	0.0720
37.60	21.67	0.16	42.3	-0.7959	1.3359	6.2500	0.0461
43.91	15.67	0.28	64.3	-0.5528	1.1951	3.5714	0.0638
57.17	23.96	0.33	58.0	-0.4815	1.3795	3.0303	0.0417
57.58	24.69	0.33	56.9	-0.4815	1.3925	3.0303	0.0405

Table 46: Pb Adsorption by Snail shell Carbonized at 600°C and Activated with HCl.

C_o(mg/l)	C_e (mg/l)	q_e (mg/g)	E (%)	$\log q_e$	$\log C_e$	$1/q_e$	$1/C_e$
35.70	17.74	0.18	50.3	-0.7447	1.2489	5.5556	0.0564
37.60	18.46	0.19	50.9	-0.7212	1.2662	5.2632	0.0542
43.91	29.14	0.14	35.9	-0.8539	1.4685	7.1429	0.0340
57.17	33.46	0.24	41.4	-0.6198	1.5425	4.1667	0.0299
57.58	30.67	0.27	46.5	-0.5686	1.4867	3.7037	0.0326

Table 47: Pb Adsorption by Snail shell Carbonized at 600°C and Activated with H_3PO_4.

C_o(mg/l)	C_e (mg/l)	q_e (mg/g)	E (%)	$\log q_e$	$\log C_e$	$1/q_e$	$1/C_e$
35.70	16.67	0.19	53.3	-0.7212	1.2219	5.2632	0.0600
37.60	28.13	0.09	25.2	-1.0458	1.4492	11.1111	0.0355
43.91	32.92	0.11	25.0	-0.9586	1.5175	9.0909	0.0304
57.17	44.80	0.12	21.6	-0.9208	1.6513	8.3333	0.0223
57.58	45.60	0.12	20.5	-0.9208	1.6590	8.3333	0.0219

Table 48: Pb Adsorption by Snail shell Carbonized at 600°C and Activated with H_2SO_4.

C_o(mg/l)	C_e (mg/l)	q_e (mg/g)	E (%)	$\log q_e$	$\log C_e$	$1/q_e$	$1/C_e$
35.70	32.1	0.04	10.0	-1.3979	1.5065	25.0000	0.0312
37.60	30.5	0.07	18.9	-1.1549	1.4843	14.2857	0.0328
43.91	35.7	0.08	18.7	-1.0969	1.5527	12.5000	0.0280
57.17	46.6	0.11	18.4	-0.9586	1.6684	9.0901	0.0215
57.58	47.4	0.09	17.3	-1.0458	1.6758	11.1111	0.0211

Table 49: Pb Adsorption by Snail shell Carbonized at 800°C and Activated with HCl.

C_o(mg/l)	C_e (mg/l)	q_e (mg/g)	E (%)	$\log q_e$	$\log C_e$	$1/q_e$	$1/C_e$
35.70	31.40	0.04	12.0	-1.3979	1.4969	25.0000	0.0318
37.60	28.16	0.09	25.1	-1.0458	1.4496	11.1111	0.0355
43.91	38.22	0.06	12.9	-1.2218	1.5823	16.6667	0.0262
57.17	52.67	0.05	7.9	-1.3010	1.7216	20.0000	0.0190
57.58	49.91	0.07	13.0	-1.1549	1.6982	14.2857	0.0200

Table 50: Pb Adsorption by Snail shell Carbonized at 800°C and Activated with H_3PO_4.

C_o(mg/l)	C_e (mg/l)	q_e (mg/g)	E (%)	$\log q_e$	$\log C_e$	$1/q_e$	$1/C_e$
35.70	33.6	0.02	5.9	-1.6990	1.5263	50.0000	0.0298
37.60	29.9	0.08	20.4	-1.0969	1.4757	12.5000	0.0334
43.91	41.6	0.02	5.2	-1.6990	1.6191	50.0000	0.0240
57.17	50.10	0.07	12.3	-1.1549	1.6998	14.2857	0.0200
57.58	51.67	0.06	9.9	-1.2218	1.7132	16.6667	0.0194

Table 51: Pb Adsorption by Snail shell Carbonized at 800°C and Activated with H_2SO_4.

C_o(mg/l)	C_e (mg/l)	q_e (mg/g)	E (%)	logq_e	logC_e	1/q_e	1/C_e
53.66	50.87	0.03	5.2	-1.5229	1.7065	33.3333	0.0197
53.06	51.65	0.01	2.7	-2.0000	1.7131	100.00	0.0194
53.90	50.59	0.03	6.1	-1.5229	1.7041	33.3333	0.0198
55.7	51.67	0.04	7.2	-1.3979	1.7132	25.0000	0.0194
57.47	54.27	0.03	5.6	-1.5229	1.7346	33.3333	0.0184

Table 52: Cd Adsorption by Snail shell Carbonized at 600°C and Activated with HCl.

C_o(mg/l)	C_e (mg/l)	q_e (mg/g)	E (%)	logq_e	logC_e	1/q_e	1/C_e
53.66	51.89	0.02	3.3	-1.6990	1.7151	50.0000	0.0193
53.06	49.91	0.03	5.9	-1.5229	1.6982	33.3333	0.2000
53.90	48.87	0.05	7.5	-1.3010	1.6980	20.0000	0.0205
55.7	53.19	0.03	4.5	-1.5229	1.7258	33.3333	0.0188
57.47	50.99	0.06	11.3	-1.2218	1.7075	16.6667	0.0196

Table 53: Cd Adsorption by Snail shell Carbonized at 600°C and Activated with H_3PO_4.

C_o(mg/l)	C_e (mg/l)	q_e (mg/g)	E (%)	logq_e	logC_e	1/q_e	1/C_e
53.66	52.10	0.02	2.9	-1.6990	1.7168	50.0000	0.0192
53.06	51.30	0.02	3.3	-1.6990	1.7101	50.0000	0.0195
53.90	50.23	0.04	6.8	-1.3979	1.7010	25.0000	0.0199
55.7	54.89	0.01	1.5	-2.0000	1.7395	100.0000	0.0182
57.47	53.67	0.04	6.6	-1.3979	1.7297	25.0000	0.0186

Table 54: Cd Adsorption by Snail shell Carbonized at 600°C and Activated with H_2SO_4.

C_o(mg/l)	C_e (mg/l)	q_e (mg/g)	E (%)	logq_e	logC_e	1/q_e	1/C_e
53.66	51.67	0.02	3.7	-1.6990	1.7132	50.0000	0.0194
53.06	50.28	0.03	5.2	-1.5229	1.7014	33.3333	0.0199
53.90	49.88	0.04	7.5	-1.3979	1.6979	25.0000	0.0200
55.70	53.82	0.02	3.4	-1.6990	1.7309	50.0000	0.0186
57.47	55.96	0.02	2.6	-1.6990	1.7479	50.0000	0.0179

Table 55: Cd Adsorption by Snail shell Carbonized at 800°C and Activated with HCl.

C_o(mg/l)	C_e (mg/l)	q_e (mg/g)	E (%)	logq_e	logC_e	1/q_e	1/C_e
53.66	49.92	0.04	7.0	-1.3979	1.6895	25.0000	0.0200
53.06	51.28	0.02	3.4	-1.6990	1.7099	50.0000	0.0195
53.90	51.22	0.03	5.0	-1.5229	1.7094	33.3333	0.0195
55.7	53.91	0.02	3.2	-1.6990	1.7317	50.0000	0.0185
57.47	56.89	0.01	1.0	-2.0000	1.7550	100.0000	0.0176

Table 56: Cd Adsorption by Snail shell Carbonized at 800°C and Activated with H_3PO_4.

C_o(mg/l)	C_e (mg/l)	q_e (mg/g)	E (%)	logq_e	logC_e	1/q_e	1/C_e
53.66	52.19	0.01	2.7	-2.0000	1.7176	100.0000	0.0192
53.06	51.92	0.01	2.1	-2.0000	1.7153	100.0000	0.0193
53.90	50.55	0.03	6.2	-1.5229	1.7307	33.3333	0.0198
55.70	51.24	0.04	6.9	-1.3979	1.7147	25.0000	0.0193
57.47	55.32	0.02	3.7	-1.6990	1.7429	50.0000	0.0181

Table 57: Cd Adsorption by Snail shell Carbonized at 800°C and Activated with H_2SO_4.

model suggests that sorption occurs on homogeneous surface by monolayer sorption without interaction between sorbed ions. Table 66 presents the determination coefficients, the Langmuir constants after experimental data were fitted. The values of b and Q° were evaluated from the intercepts and slopes respectively for the 24 types of OBAC. It was deduced from the table that the coefficient of determinations were all poorly fitted into the Langmuir model equation except for few of them. The range of the R^2 values was 0.00 to 0.993 with most falling below 0.500.

C_o(mg/l)	C_e (mg/l)	q_e (mg/g)	E (%)	logq_e	logC_e	1/q_e	1/C_e
75.05	8.48	0.67	88.7	-0.1739	0.9284	1.4925	0.1179
114.69	112.51	0.02	1.9	-1.6990	2.0512	50.0000	0.0089
135.24	133.19	0.02	4.5	-1.6990	2.1245	50.0000	0.0075
145.14	75.63	0.69	47.9	-0.1612	1.8787	1.4493	0.0132
147.28	145.12	0.02	1.47	-1.6990	2.1617	50.0000	0.0689

Table 58: Mn Adsorption by Snail shell Carbonized at 600°C and Activated with HCl.

C_o(mg/l)	C_e (mg/l)	q_e (mg/g)	E (%)	logq_e	logC_e	1/q_e	1/C_e
75.05	0.88	0.74	98.8	-0.1308	-0.0555	1.3514	1.1364
114.69	7.47	1.07	93.4	0.0294	0.8733	0.9346	0.1339
135.24	19.58	1.16	85.5	0.0645	1.2918	0.8621	0.0511
145.14	11.95	1.33	91.8	0.1239	1.0774	0.7519	0.0837
147.28	46.45	1.00	68.4	0.0000	1.6670	1.0000	0.0215

Table 59: Mn Adsorption by Snail shell Carbonized at 600°C and Activated with H_3PO_4.

C_o(mg/l)	C_e (mg/l)	q_e (mg/g)	E (%)	logq_e	logC_e	1/q_e	1/C_e
75.05	2.16	0.73	97.1	-0.1367	0.3345	1.3699	0.4630
114.69	3.57	1.11	96.9	0.0453	0.5527	0.9009	0.2801
135.24	12.55	1.23	90.7	0.0899	1.0986	0.8130	0.0797
145.14	26.19	1.19	81.9	0.0755	1.4181	0.8403	0.0382
147.28	57.8	0.89	60.8	-0.0506	1.7619	1.1236	0.0173

Table 60: Mn Adsorption by Snail shell Carbonized at 600°C and Activated with H_2SO_4.

C_o(mg/l)	C_e (mg/l)	q_e (mg/g)	E (%)	logq_e	logC_e	1/q_e	1/C_e
75.05	69.91	0.05	6.8	-1.3010	1.8445	20.0000	0.0143
114.69	111.32	0.03	2.9	-1.5229	2.0466	33.3333	0.0090
135.24	128.77	0.06	4.8	-1.2218	2.1098	16.6667	0.0078
145.14	141.87	0.03	2.3	-1.5229	2.1519	33.3333	0.0070
147.28	146.00	0.01	0.9	-2.0000	2.1647	100.0000	0.0068

Table 61: Mn Adsorption by Snail shell Carbonized at 800°C and Activated with HCl.

C_o(mg/l)	C_e (mg/l)	q_e (mg/g)	E (%)	logq_e	logC_e	1/q_e	1/C_e
75.05	70.38	0.05	6.2	-1.3010	1.8474	20.0000	0.0142
114.69	109.40	0.05	4.6	-1.3010	2.0390	20.0000	0.0091
135.24	128.37	0.07	5.1	-1.1549	2.1085	14.2857	0.0078
145.14	133.88	0.11	7.8	-0.9586	2.1267	9.0909	0.0075
147.28	140.76	0.07	4.4	-1.1549	2.1485	14.2857	0.0071

Table 62: Mn Adsorption by Snail shell Carbonized at 800°C and Activated with H_3PO_4.

C_o(mg/l)	C_e (mg/l)	q_e (mg/g)	E (%)	logq_e	logC_e	1/q_e	1/C_e
75.05	67.89	0.07	9.5	-1.1549	1.8318	14.2857	0.0147
114.69	109.48	0.05	4.5	-1.3010	2.0393	20.0000	0.0091
135.24	121.36	0.14	10.2	-0.8539	2.0841	7.1429	0.0082
145.14	136.55	0.09	5.9	-1.0458	2.1353	11.1111	0.0073
147.28	146.75	0.01	0.4	-2.0000	2.1666	100.0000	0.0068

Table 63: Mn Adsorption by Snail shell Carbonized at 800°C and Activated with H_2SO_4.

The essential characteristics of Langmuir isotherm can be expressed in terms of a dimensionless equilibrium parameter (R_L) called Separation Factor [19], which is defined as:

R_L=1/(1+bCo)

Where b=Langmuir constant and Co is the highest initial metal concentration (mg/l).

S/N	AC Type	Equation	R^2	n	K_f
1	Ni OBAC 600°C HCl	Y=-0.064x-0.205	0.603	15.6	1.6
2	Ni OBAC 600°C H_2SO_4	Y=-0.077x-0.247	0.693	12.9	1.8
3	Ni OBAC 600°C H_3PO_4	Y=-0.524x+0.203	0.901	1.91	1.6
4	Ni OBAC 800°C HCl	Y=-0.881x+0.402	0.739	1.14	2.5
5	Ni OBAC 800°C H_2SO_4	Y=-0.074x-0.465	0.001	13.5	2.9
6	Ni OBAC 800°C H_3PO_4	Y=-0.881x+0.402	0.739	1.14	2.5
7	Cd OBAC 600°C HCl	Y=-1.723x+1.729	0.917	0.58	53.6
8	Cd OBAC 600°C H_2SO_4	Y=-0.881x+0.402	0.739	1.14	2.5
9	Cd OBAC 600°C H_3PO_4	Y=-1.586x+1.634	0.999	0.63	43.1
10	Cd OBAC 800°C HCl	Y=-1.325x+1.114	0.815	0.75	13.0
11	Cd OBAC 800°C H_2SO_4	Y=-4.274x+5.882	0.934	0.23	$7.6x10^5$
12	Cd OBAC 800°C H_3PO_4	Y=-0.570x+0.045	0.022	1.75	1.1
13	Pb OBAC 600°C HCl	Y=-0.881x+0.402	0.739	1.14	2.5
14	Pb OBAC 600°C H_2SO_4	Y=1.243x-3.190	0.388	0.80	1.5
15	Pb OBAC 600°C H_3PO_4	Y=1.745x-3.681	0.727	0.57	$4.7x10^3$
16	Pb OBAC 800°C HCl	Y=0.224x-3.190	0.939	4.46	2.2
17	Pb OBAC 800°C H_2SO_4	Y=0.034x-0.319	0.089	29.4	2.1
18	Pb OBAC 800°C H_3PO_4	Y=0.216x-0.383	0.985	4.63	2.4
19	Mn OBAC 600°C HCl	Y=2.394x-5.693	0.422	0.42	$4.9x10^5$
20	Mn OBAC 600°C H_2SO_4	Y=-0.031x-1.195	0.001	32.3	15.7
21	Mn OBAC 600°C H_3PO_4	Y=-0.624x-2.281	0.132	1.6	191
22	Mn OBAC 800°C HCl	Y=-0.349x+0.307	0.826	2.87	2.0
23	Mn OBAC 800°C H_2SO_4	Y=-0.487x+0.524	0.479	2.05	3.3
24	Mn OBAC 800°C H_3PO_4	Y=-0.220x-0.012	0.366	4.55	1.0

Table 64: Freundlich Adsorption Isotherm Constants for Oil Bean Activated Carbon.

S/N	AC Type	Equation	R^2	n	K_f
1	Ni SSAC 600°C HCl	Y=-1.440x+0.944	0.057	0.69	8.8
2	Ni SSAC 600°C H_3PO_4	Y=-0.934x+0.285	0.098	1.07	1.9
3	Ni SSAC 600°C H_2SO_4	Y=-4.309x+6.011	0.710	0.23	1.0×10^6
4	Ni SSAC 800°C HCl	Y=-3.636x+4.919	0.927	0.28	8.2×10^4
5	Ni SSAC 800°C H_3PO_4	Y=2.648x-5.995	0.455	0.38	9.8×10^5
6	Ni SSAC 800°C H_2SO_4	Y=-1.832x+1.847	0.175	0.55	70.3
7	Pb SSAC 600°C HCl	Y=0.346x-1.040	0.085	2.89	11.0
8	Pb SSAC 600°C H_3PO_4	Y=0.299x-1.121	0.131	3.34	13.2
9	Pb SSAC 600°C H_2SO_4	Y=-0.387x-0.331	0.341	2.58	2.1
10	Pb SSAC 800°C HCl	Y=1.375x-3.300	0.555	0.73	1995.3
11	Pb SSAC 800°C H_3PO_4	Y=-0.200x-0.906	0.031	5.0	8.1
12	Pb SSAC 800°C H_2SO_4	Y=0.511x-2.196	0.031	1.96	157.0
13	Cd SSAC 600°C HCl	Y=0.750x-2.879	0.001	1.33	756.8
14	Cd SSAC 600°C H_3PO_4	Y=-7.042x+10.58	0.188	0.14	3.8×10^{10}
15	Cd SSAC 600°C H_2SO_4	Y=-9.019x+13.86	0.301	0.11	7.2×10^{13}
16	Cd SSAC 800°C HCl	Y=-5.162x-7.266	0.817	0.19	1.8×10^7
17	Cd SSAC 800°C H_3PO_4	Y=-8.562x+13.05	0.890	0.12	1.1×10^{13}
18	Cd SSAC 800°C H_2SO_4	Y=4.88wx-10.14	0.048	0.20	1.3×10^{10}
19	Mn SSAC 600°C HCl	Y=-1.222x+1.149	0.563	0.82	14.1
20	Mn SSAC 600°C H_3PO_4	Y=0.099x-0.079	0.457	10.10	1.2
21	Mn SSAC 600°C H_2SO_4	Y=0.051x-0.048	0.099	19.61	1.1
22	Mn SSAC 800°C HCl	Y=-1.221x+0.986	0.273	0.82	9.7
23	Mn SSAC 800°C H_3PO_4	Y=0.776x-2.768	0.456	1.29	586.1
24	Mn SSAC 800°C H_2SO_4	Y=-1.097x+0.981	0.109	0.91	9.6

Table 65: Freundlich Adsorption Isotherm Constants for Snail Shell Activated Carbon.

The value of R_L indicates the type of the isotherm to be either unfavourable ($R_L>1$), linear ($R_L=1$), favourable ($0<R_L<1$) or irreversible ($R_L=0$).

The Langmuir isotherm model for the adsorption of Ni, Pb, Cd and Mn on OBAC generally had low determination coefficients (Table 66). It shows that the Langmuir isotherm plot did not have a good fit in most of the plots. Though the determination coefficient was low, the essential characteristics of Langmuir isotherm (separation factor) R_L, showed that the isotherm were all favourable except for that of Pb/OBAC/800°C/H_2SO_4 which had a zero separation factor and this means the isotherm is irreversible ($R_L=0$) [19].

The Langmuir adsorption constants were generally high indicating

S/N	AC Type	Equation	R^2	Q^o	b (l/mg)	R_L
1	Ni OBAC 600°C HCL	Y=-1.181x+2.562	0.249	0.8467	0.460	0.032
2	Ni OBAC 600°C H_2SO_4	Y=-0.707x+2.224	0.477	1.4144	0.320	0.045
3	Ni OBAC 600°C H_3PO_4	Y=-30.75x+45.216	0.861	0.0330	5.895	0.003
4	Ni OBAC 800°C HCL	Y=-83.78x+14.88	0.213	0.0120	5.600	0.003
5	Ni OBAC 800°C H_2SO_4	Y=3.005x+3.746	0.000	0.3300	0.800	0.018
6	Ni OBAC 800°C H_3PO_4	Y=-287.9x+16.26	0.82	0.0035	17.70	0.0008
7	Cd OBAC 600°C HCL	Y=-392.0x+24.60	0.657	0.0026	15.90	0.001
8	Cd OBAC 600°C H_2SO_4	Y=-0.205x+2.208	0.440	4.9000	0.090	0.162
9	Cd OBAC 600°C H_3PO_4	Y=-314.7x+17.19	0.993	0.0032	18.30	0.0009
10	Cd OBAC 800°C HCL	Y=-219.6x+19.34	0.490	0.0046	11.40	0.002
11	Cd OBAC 800°C H_2SO_4	Y=-3067x+91.90	0.717	0.00033	3.300	0.008
12	Cd OBAC 800°C H_3PO_4	Y=2.351x+2.142	0.348	0.4000	1.100	0.005
13	Pb OBAC 600°C HCL	Y=565.4x-1.306	0.706	0.0018	432.9	0.00004
14	Pb OBAC 600°C H_3PO_4	Y=617.8x-9.650	0.385	0.0016	64.00	0.0003
15	Pb OBAC 600°C H_2SO_4	Y=628.9x+1.756	0.250	0.0016	570.7	0.00003
16	Pb OBAC 800°C HCL	Y=0.374x+1.677	0.885	2.7000	0.200	0.080
17	Pb OBAC 800°C H_3PO_4	Y=0.536x+1.756	0.950	1.9000	0.300	0.055
18	Pb OBAC 800°C H_2SO_4	Y=0.000x+2.241	0.004	0.000	0.000	0.000
19	Mn OBAC 600°C HCL	Y=1748x-7.473	0.319	0.00057	233.9	0.00002
20	Mn OBAC 600°C H_3PO_4	Y=467.2x+6.811	0.066	0.0021	68.60	0.00009
21	Mn OBAC 600°C H_2SO_4	Y=-121.8x+19.63	0.008	0.0082	6.200	0.001
22	Mn OBAC 800°C HCL	Y=-12.26x+2.594	0.892	0.0820	4.700	0.001
23	Mn OBAC 800°C H_3PO_4	Y=-1.940x+3.125	0.168	0.5000	0.600	0.011
24	Mn OBAC 800°C H_2SO_4	Y=-54.86x+3.502	0.355	0.0180	15.70	0.0004

Table 66: Langmuir Adsorption Isotherm Constants for Oil Bean Activated Carbon.

strong adsorption intensity and as well as good adsorption capacity of the activated carbons. From observation, the two Langmuir isotherm constants seem to have an inverse relationship in most of the OBAC types except for few of them. In the Table 67 which is the summarized Langmuir isotherm model constants for snail shell activated carbon, it shows that they generally had a poor fit as most of the R^2 are below 0.500 unlike that of the OBAC. Though the adsorption capacity constant Q^o was very low, the Langmuir adsorption energy was really high. This further confirms the inverse relationship observed earlier in the Langmuir plot of the data from the snail shell activated carbon adsorption experiment. Despite the poor fit of the Langmuir plot, the adsorption was favourable considering the separation factor which is an essential characteristics of the Langmuir plot ($0<R_L<1$).

Anova for Langmuir adsorption isotherm constants

Analysis of variance (ANOVA) was conducted on the reliability factor (R^2), the Langmuir adsorption capacity Q^o and the Langmuir adsorption intensity for all the type of activated carbons produced. For OBAC, the correlation of R^2 and Q^o showed no statistically significant relation between them and so also it was for R^2 and b (sig=0.446, 0.755 respectively, $P>0.05$). For Q^o and b, the correlation was negative and insignificant as well. For SSAC, the ANOVA for Q^o and R^2 showed no significant relation but the paired samples T-test for b and Q^o showed a negative correlation indicating that as b increases, Q^o decreases. The T-test between b and R^2 showed a positive significant correlation.

Anova for Freundlich adsorption isotherm constants

For OBAC, the ANOVA showed that there was no significant relationship between R^2 and n, but a significant relationship between R^2 and K_f. The paired samples T-test showed a positive significant relationship between R^2 and n but between R^2 and K_f and n and K_f, there was no significant relationship. The correlation of R^2 and n showed a significant negative correlation ($r=-0.545$, $P<0.05$), indicating that as the value of R^2 increases, that of n increases. Between K_f and R^2, there was no significant correlation. For SSAC, the anova and correlation for R^2 and n, K_f and R^2 and K_f and n, there was no significant relation, t for the paired sample T-test, there was a significant relationship between R^2 and n.

Figure 17 shows the SEM images of char samples produced by pyrolysis of Oil Bean as activated carbon precursor at different temperatures. Comparing SEM images of the char samples produced under the two temperatures (600°C and 800°C), it can be seen that the pore development on the surfaces of the carbon were similar in their pores and the pores were not evenly distributed as well. That carbonized at 600°C developed more pores than its counterpart but that at 800°C had larger pore size than the 600°C carbon. Looking at the Figure 18, it can be seen that activation of the carbons with acid developed more micro pores as well expanded the initial pores created during carbonization. After the activation the pores were evenly distributed especially for those carbonized at 600°C but with a rough surface (Figure 19). The SEM photograph of the snail shell activated carbon showed no visible pores. This may be as a result of presence of impurities such as tar which may have clogged the pores developed by the shell which inhibited the pores structure development (Figure 20). Table 68 shows the pore volumes of the carbons produced. The pore volumes of the activated carbons were larger than the unactivated carbons in all the type of carbon produced. The activated carbons had good pore volumes which is an indication of good adsorptive capacity except for Snail Shell activated carbons.

The observed trend for the Oil Bean activated carbon pore volume is OBAC/600°C/H_2SO_4>OBAC/800°C/H_2SO_4=OBAC/800°C/H_3PO_4>OBAC/800°C/HCl=OBAC/600°C/HCl. For Peanut Seed activated carbon is PNAC/800°C/H_3PO_4=PNAC/800°C/H_2SO_4>PNAC/800°C/HCl>PNAC/600°C/H_3PO_4=PNAC/600°C/H_2SO_4>PNAC/600°C/HCl. For Palm Kernel Shell it is PKAC 600°C HCl>PKAC/600°C/H_2SO_4>PKAC/600°C/H_3PO_4=PKAC/800°C/HCl=PKAC/800°C/H_3PO_4=PKAC/800°C/H_2SO_4. For Snail

S/N	AC Type	Equation	R^2	Q^o	b (l/mg)	R_L
1	Ni SSAC 600°C HCL	Y=-45697x+126.7	0.072	0.00020	36.30	0.00041
2	Ni SSAC 600°C H_3PO_4	Y=-1429x+46.75	0.259	0.00070	30.60	0.0004
3	Ni SSAC 600°C H_2SO_4	Y=-1041x+222.1	0.551	0.000099	45.20	0.00033
4	Ni SSAC 800°C HCL	Y=-4098x+105.2	0.800	0.00024	39.00	0.00038
5	Ni SSAC 800°C H_3PO_4	Y=3221x-33.24	0.414	0.00031	96.90	0.00015
6	Ni SSAC 800°C H_2SO_4	Y=-8905x+41.38	0.029	0.00011	215.2	0.00006
7	Pb SSAC 600°C HCL	Y=16.52x+3.212	0.029	0.06000	5.100	0.0034
8	Pb SSAC 600°C H_3PO_4	Y=25.74x+4.1	0.060	0.03900	6.300	0.0028
9	Pb SSAC 600°C H_2SO_4	Y=-80.44x+11.16	0.356	0.01200	7.200	0.0024
10	Pb SSAC 800°C HCL	Y=772.0x-6.385	0.451	0.00130	120.9	0.00014
11	Pb SSAC 800°C H_3PO_4	Y=-263.2x+25.59	0.105	0.00380	10.30	0.0017
12	Pb SSAC 800°C H_2SO_4	Y=560.5x+14.49	0.031	0.00180	38.70	0.0005
13	Cd SSAC 600°C HCL	Y=2840x-9.943	0.002	0.00035	28.50	0.00006
14	Cd SSAC 600°C H_3PO_4	Y=17.79x+29.67	0.011	0.05600	0.600	0.0282
15	Cd SSAC 600°C H_2SO_4	Y=-28105x+586.2	0.393	0.000036	47.90	0.0004
16	Cd SSAC 800°C HCL	Y=-10378x+240.5	0.622	0.000096	43.20	0.0004
17	Cd SSAC 800°C H_3PO_4	Y=-27913x+582.5	0.852	0.000035	47.90	0.00036
18	Cd SSAC 800°C H_2SO_4	Y=-2544x+110.3	0.001	0.00039	23.10	0.0008
19	Mn SSAC 600°C HCL	Y=-225.1x+40.33	0.172	0.00440	5.600	0.0012
20	Mn SSAC 600°C H_3PO_4	Y=0.428x+0.857	0.813	2.33640	0.500	0.0134
21	Mn SSAC 600°C H_2SO_4	Y=0792x+0.870	0.415	1.36200	0.900	0.0075
22	Mn SSAC 800°C HCL	Y=-5124x+86.68	0.217	0.00020	59.10	0.0001
23	Mn SSAC 800°C H_3PO_4	Y=1086x+5.604	0.478	0.00092	193.8	0.00004
24	Mn SSAC 800°C H_2SO_4	Y=-4793x+74.7	0.152	0.00021	64.20	0.00010

Table 67: Langmuir Adsorption Isotherm Constants for Snail Shell Activated Carbon.

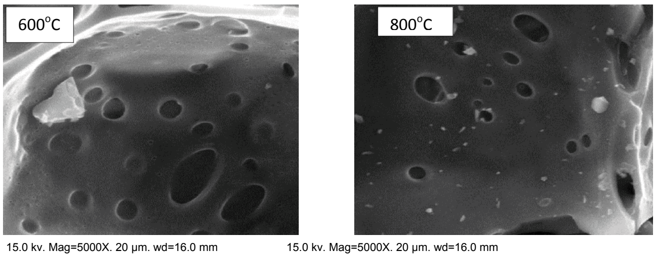

Figure 17: SEM image of Oil Bean Carbonised at 600°C and 800°C.

Shell activated carbon it is SSAC/600°C HCl>SSAC/800°C/HCl>SSAC/800°C/H_2SO_4>SSAC/800°C/H_3PO_4>SSAC/600°C/H_3PO_4>SSAC/600°C/H_2SO_4. Larger pore volumes are advantageous in removing larger heavy metals from aqueous media (Table 68).

Conclusions

The result of these studies shows that it is possible to prepare activated carbon from oil bean shell, peanut seed, palm kernel shell and snail shell and they can be used effectively in the treatment of wastewater from industries. The precursors are common in these parts of the world and they are cheap to obtain since they are waste generated from their consumption. The proximate analysis of the different precursors reveals that they are effective in the treatment of wastewater since they can easily be homogenized into fine granules and powder as well giving it a large surface area for adsorption. The precursors had good percentage yield after activation at both experimental temperature used. The activated carbon produced showed good adsorption capacity for the industrial waste. The FTIR analysis indicates that there was a reorganization of the chemical bonds present in the surfaces of the activated carbons. This may be attributed to the presence of oxygen atoms on the surface of the activated carbons. For the percentage adsorption of heavy metals by the activated carbon, Oil Bean carbonized at 600°C was better adsorbent for the adsorption of Ni and Cd but for Pb and Mn, it was those carbonized at 800°C that were better off. A similar result was observed for snail shell activated carbon were Pb, Cd and Mn adsorption was better with those carbonized at 600°C unlike Ni adsorption by Snail Shell activated carbon. It was observed that those carbon activated with H_3PO_4 were better adsorbents in most of the activated carbons produced irrespective of the heavy metals,

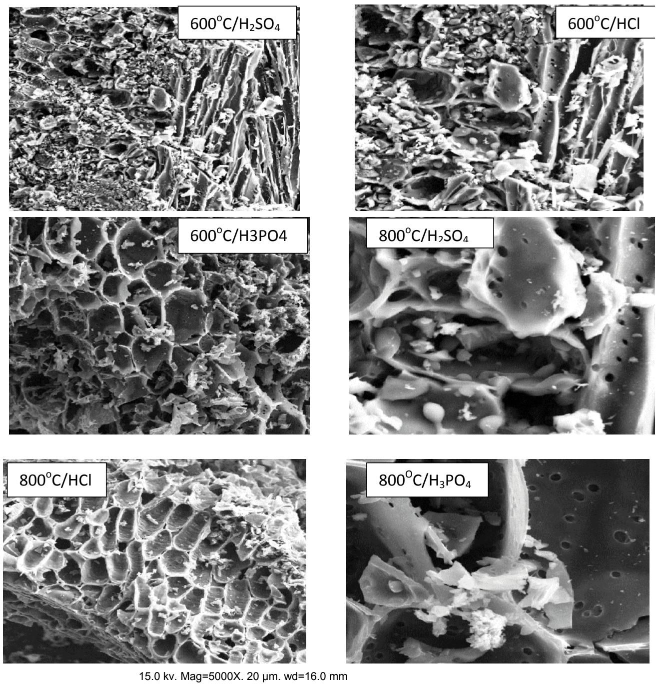

Figure 18: SEM image of Oil Bean Carbonised at 600°C and 800°C and Activated with acids.

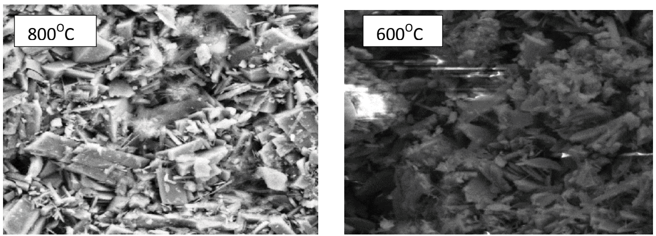

15.0 kv. Mag=5000 X. 20 µm. wd=16.0 mm

Figure 19: SEM image of Snail Shell Carbonised at 600°C and 800°C.

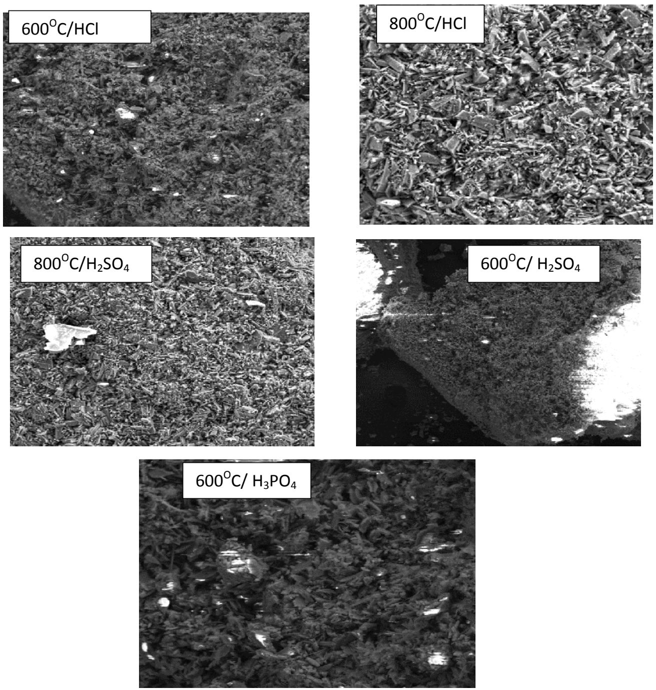

15.0 kv. Mag=5000X. 20 µm. wd=16.0 mm

Figure 20: SEM image of Snail Shell Carbonised at 600°C and 800°C and Activated with acids.

Activated Carbon Type	Pore Volume (m^3/g)
OBAC 600°C	3.9×10^{-5}
OBAC 800°C	3.5×10^{-5}
OBAC 600°C HCl	2.9×10^{-5}
OBAC 600°C H_2SO_4	2.4×10^{-5}
OBAC 600°C H_3PO_4	2.6×10^{-5}
OBAC 800°C HCl	2.9×10^{-5}
OBAC 800°C H_2SO_4	2.5×10^{-5}
OBAC 800°C H_3PO_4	2.5×10^{-5}
SSAC 800°C	7.9×10^{-6}
SSAC 600°C HCl	6.2×10^{-6}
SSAC 600°C H_3PO_4	7.1×10^{-6}
SSAC 600°C H_2SO_4	7.3×10^{-6}
SSAC 800°C HCl	6.7×10^{-6}
SSAC 800°C H_3PO_4	6.9×10^{-6}
SSAC 800°C H_2SO_4	6.8×10^{-6}

Table 68: Pore Volume of both activated and unactivated carbons.

followed by those activated with HCl while those activated with H_2SO_4 were the least. The experimental adsorption data fitted well on the Freundlich isotherm model much better than the Langmuir isotherm model indicating heterogeneous surface energies which gives an exponential distribution of active sites. In most of the activated carbon types, the adsorption intensities were greater than one indicating also a favourable adsorption. So also it was for the adsorption capacities. This fact is supported by the values of the separation factors R_L. The ANOVA indicates that there exist a positive significance relationship between the reliability factor (R^2) and the Langmuir constants in almost all the activated carbon types produced. So also it was for Freundlich isotherm constants except few of them. There was a great effect of the chemical activation process on the pore development in virtually all the activated carbon types produced as shown by the pore volumes of the AC indicated by both before and after activation.

References

1. Fitzgerald WF, Engstrom DR, Mason RP, Nater EA (1998) The case for atmospheric mercury contamination in remote areas. Environ Sci Technol 32: 1-7.
2. Babut M, Sekyi R, Rambaud A, Gautier PM, Tellier S, et al. (2003) Improving the environmental management of small-scale gold mining in Ghana: a case study of Dumasi. Journal of Cleaner Production 11: 215-221.
3. Grigis BS, Ishak MF (1999) Activated carbon from cotton stalks by Impregnated with phosphoric acid. Material Letters 39: 107-114.
4. AOAC (1984) Official methods of analysis: Association of official analytical Chemists. 14th edn. Washington DC.
5. Adrian WJA (1973) Comparison of a wet pressure digestion method with other commonly used wet and dry-ashing methods. Analyst 98: 213-216.
6. APHA (1998) Standard Methods for the Examination of Water and Wastewater. American Public Health Association, Washington, DC, New York, USA.
7. Daud WMAW, Ali WSW (2004) Comparison on pore development of activated carbon produced from palm shell and coconut shell. Bioresource Technology 93: 63-69.
8. Ademiluyi FT, David-West EO (2012) Effect of Chemical Activation on the Adsorption of Heavy Metals Using Activated Carbons from Waste Materials. International Scholarly Research Network (ISRN) Chemical Engineering: 5.
9. Abechi SE, Gimba CE, Uzairu A, Dallatu YA (2013) Preparation and characterization of Activated carbon from Palm Kernel shell by chemical activation. Research Journal of chemical sciences 3: 54-61.
10. Nale BY, Kagbu JA, Uzairu A, Nwankwere ET, Saidu S, et al. (2012) Kinetic and Equilibrium studies of the adsorption of Lead (II) and Nickel(II) ions from aqueous solutions on activated carbon prepared from Maize Cob. Pelagia Research Library 3: 302-312.
11. Huang GF, Wu QT, Wong JWC, Nagar BB (2005) Transformation of organic matter during co-composting of pig manure with sawdust. Bioresources Technology 35: 132-137.
12. Zawadzki J (1989) Chemistry and Physics of Carbon, Vol Marcel Dekker, Inc., New York.
13. McEnaney B, Mays TJ (1989) Introduction to Carbon Science. Butterworths, London.
14. Yakubu M, Gumel K, Abdullah MS (2008) Use of activated carbon from date seeds to treat textile and tannery effluents. African Journal of Science and Technology 9: 31-40 .
15. Uddin MT, Islam MS, Abedin MZ (2007) Adsorption of phenol from aqueous solution by water hyacinth ash. ARPN J of Engineering and Applied Sciences 2: 121-128.
16. Okeola, Odebunmi FO, Freundlich EO (2010) Langmuir Isotherm Parameters for Adsorption of Methylene Blue by Activated Carbon Derived from Agrowastes. Advances in Natural and Applied Sciences 4: 281-288.
17. Zaid Ahmed AA, Mohammed AS (2008) Thermodynamics and Kinetics Studies of Iron (III) Adsorption by Olive Cake in a Batch System. J Mex Chem Soc 52: 108-115.
18. Abdul HA, Yussof MS, Adlan MN, Adnan NH, Salina Alias (2003) Physico-chemical removal of iron from semi-aerobic landfill leachate by limestone filter. Waste Management 24: 353-358.
19. Hall KR, Eagleton LC, Acrivos A, Vermeulen T (1966) Pore and solid diffusion kinetic in fixed bed adsorption under constant pattern conditions. Industrial and engineering chemistry fundamentals 5: 212-223.